energie atomique • energies alternatives

Low-energy dipole excitations in Neon isotopes and N=16 isotones

Marco Martini
CEA/DAM/DIF

in collaboration with Sophie Péru and Marc Dupuis

energie atomique • energies alternatives

Dipole excitations

Giant Dipole Resonance (GDR)

- Typical of all nuclei
- Known since more than 60 years
- Very collective response
- Isovector

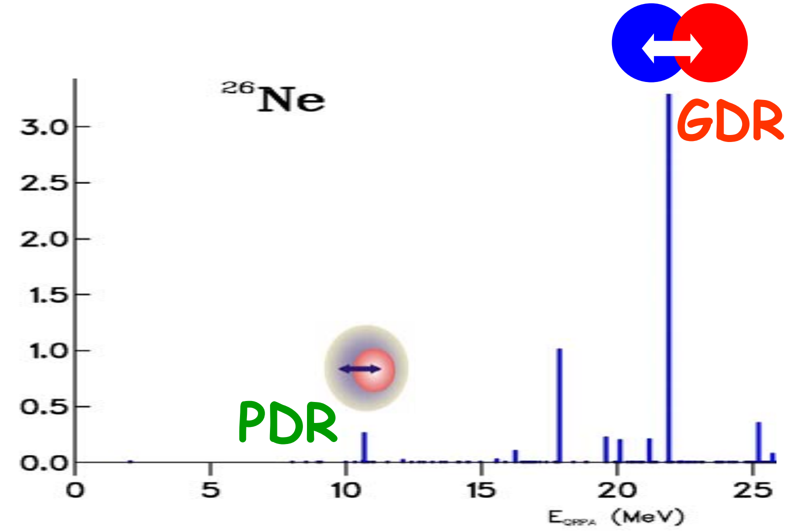

Low energy, Pygmy (PDR)

- In nuclei with neutron-proton asymmetry
- Known since the end of '80
- ^{6,8}He, ^{11}Li, ^{11,12,14}Be, ^{15,17,19}C, $^{17-22}$O, ^{26}Ne, ^{44,48}Ca, ^{56}Fe, ^{58}Ni, ^{88}Sr, ^{112}Sn, ^{116,124}Sn, isotones N=82: ^{138}Ba, ^{140}Ce, ^{142}Nd, ^{144}Sm; ^{204,206,207,208}Pb

- What's the dynamics?
- Degree of collectivity?
- Isoscalar or isovector?
- Evolution with neutron proton asymmetry?
- New opportunities with the advent of radioactive beams

Radiative neutron captures

Maxwellian-averaged (n,γ) rates

Some percent of E1 strength due to the PDR is sufficient to appreciably increase the neutron capture cross section σ (n,γ).

e.g. 1% of the total E1 strength at E_{PDR}=4.2 MeV is sufficient to increase by a factor 5 the neutron capture cross section σ (n,γ) of ^{209}Pb.

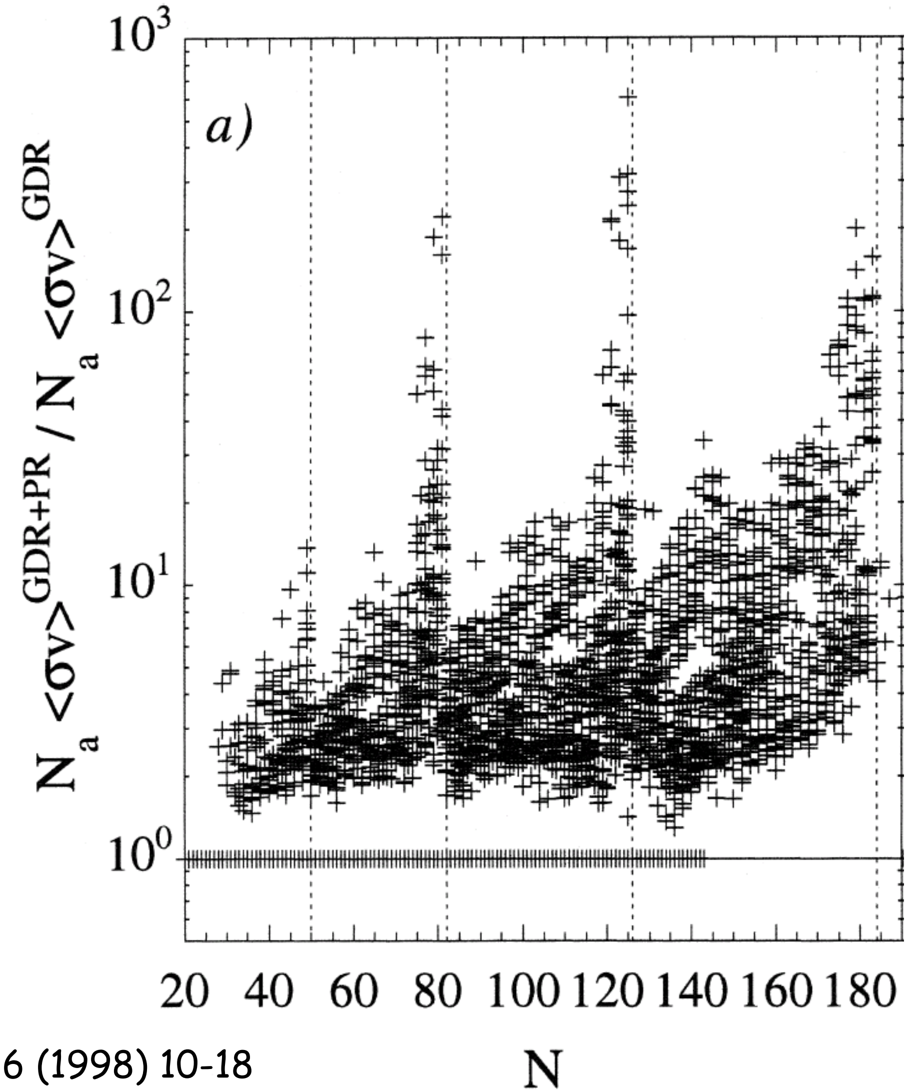

S. Goriely, Physics Letters B 436 (1998) 10-18

Large scale microscopic QRPA calculation

energie atomique • energies alternatives

(n,γ) cross section

The more microscopic the underlying theory is, the greater will be the confidence in the extrapolations towards the experimentally unreachable nuclei, provided the predictions are capable of reproducing experimentally known data with a sufficient degree of accuracy.

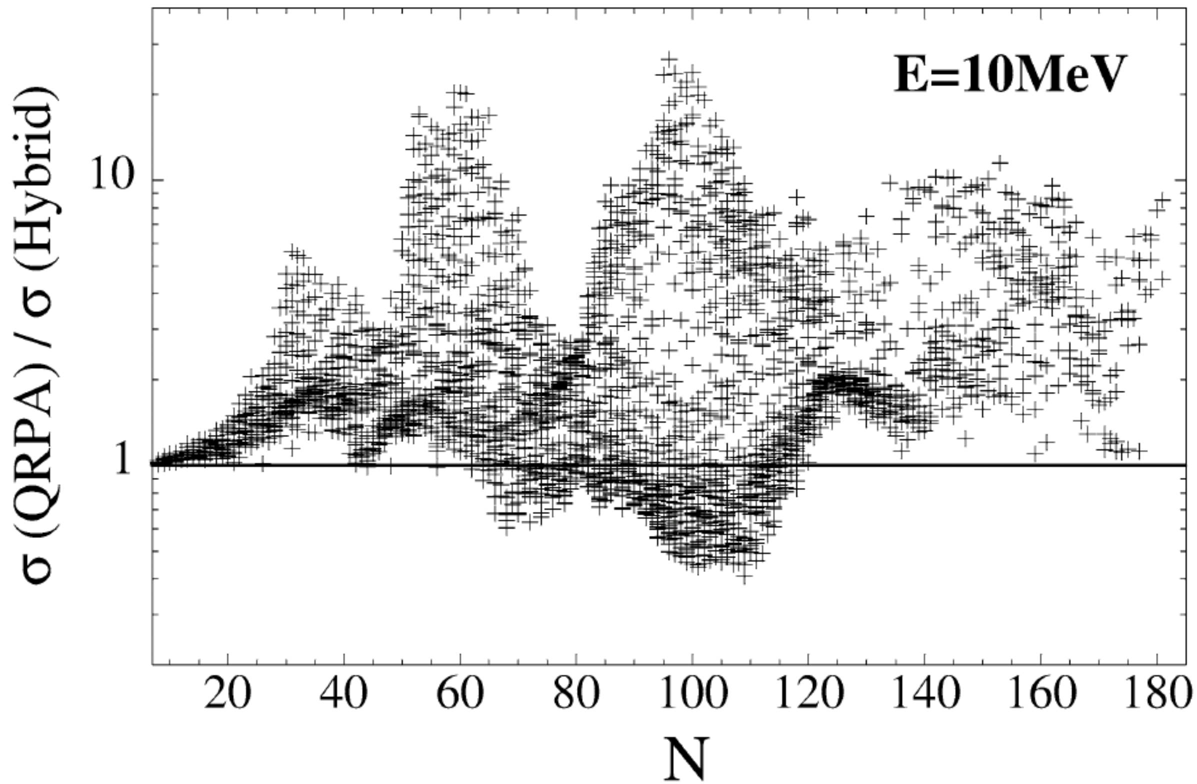

S. Goriely, E. Khan, Nuclear Physics A 706 (2002) 217-232

r (rapid)-process nucleosynthesis

energie atomique • energies alternatives

Responsible for the creation of approximately one half of the neutron-rich nuclei heavier than iron.

Rapid neutron capture at high temperature and neutron density (core-collapse supernova; two colliding neutron stars).

PDR effect tends to accelerate the neutron captures and enables the production of heavier nuclei (A~130).

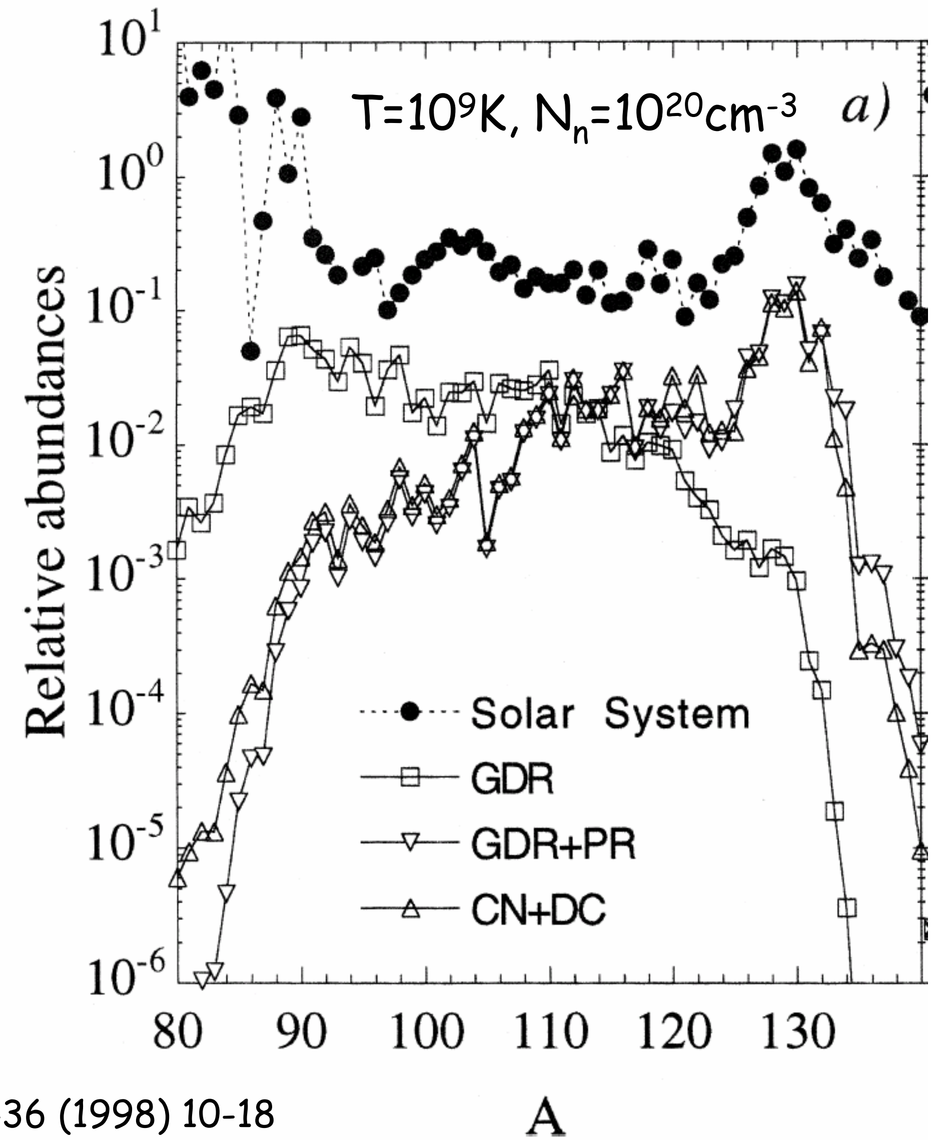

S. Goriely, Physics Letters B 436 (1998) 10-18

Correlations between PDR and symmetry energy

$$\frac{E}{A}(\rho,\delta) = \frac{E}{A}(\rho,\delta=0) + S(\rho)\delta^2$$

$$\delta \equiv (\rho_n - \rho_p)/\rho$$

$$S'(\rho)|_{\rho=\rho_0} = \frac{L}{3\rho_0}$$

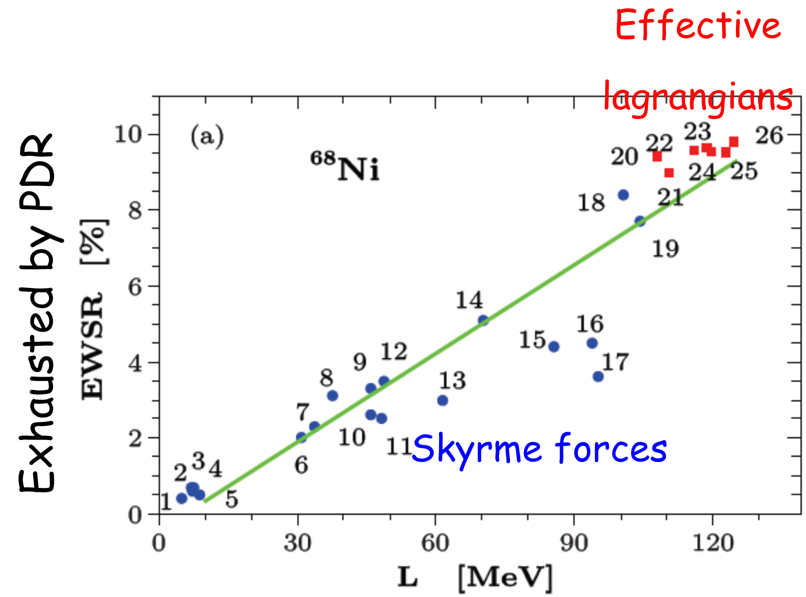

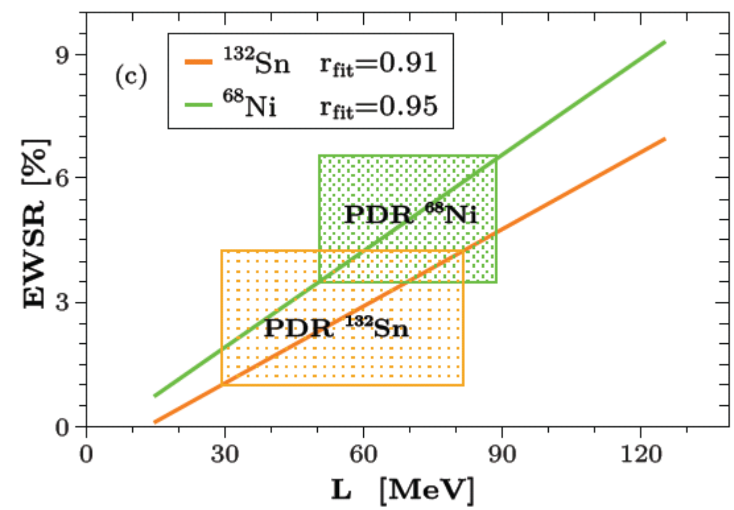

→ Isospin-dependent components of effective forces

→ Nuclear matter equation of state

→ Size of neutron r.m.s., neutron skins

Carbone et al Phys. Rev. C 81, 041301 (2010)

Why Neon isotopes et N=16 isotones in QRPA?

Low-energy dipole excitations

- Light nuclei: non-resonant independent s.p. excitations of loosly bound n
- Isotones N=82: PDR collective
- N=16?

Other microscopical calculations:

RMF-RRPA (meson exchange lagrangians), QRPA (Skyrme), Landau-Migdal

PRL **101,** 212503 (2008) PHYSICAL REVIEW LETTERS week ending 21 NOVEMBER 2008

Decay Pattern of Pygmy States Observed in Neutron-Rich ^{26}Ne

J. Gibelin,[1,2,*] D. Beaumel,[1] T. Motobayashi,[3] Y. Blumenfeld,[1] N. Aoi,[3] H. Baba,[3] Z. Elekes,[4] S. Fortier,[1] N. Frascaria,[1] N. Fukuda,[3] T. Gomi,[3] K. Ishikawa,[5] Y. Kondo,[5] T. Kubo,[3] V. Lima,[1] T. Nakamura,[5] A. Saito,[6] Y. Satou,[5] J.-A. Scarpaci,[1] E. Takeshita,[2] S. Takeuchi,[3] T. Teranishi,[7] Y. Togano,[2] A. M. Vinodkumar,[5] Y. Yanagisawa,[3] and K. Yoshida[3]

Coulomb excitation of the exotic neutron-rich nucleus ^{26}Ne on a ^{208}Pb target was measured at 58 MeV/u in order to search for low-lying $E1$ strength above the neutron emission threshold. This radioactive beam experiment was carried out at the RIKEN Accelerator Research Facility. Using the invariant mass method in the ^{25}Ne + n channel, we observe a sizable amount of $E1$ strength between 6 and 10 MeV excitation energy. By performing a multipole decomposition of the differential cross section, a reduced dipole transition probability of $B(E1) = 0.49 \pm 0.16e^2$ fm^2 is deduced, corresponding to 4.9 ± 1.6% of the Thomas-Reiche-Kuhn sum rule. For the first time, the decay pattern of low-lying strength in a neutron-rich nucleus is measured. The extracted decay pattern is not consistent with several mean-field theory descriptions of the pygmy states.

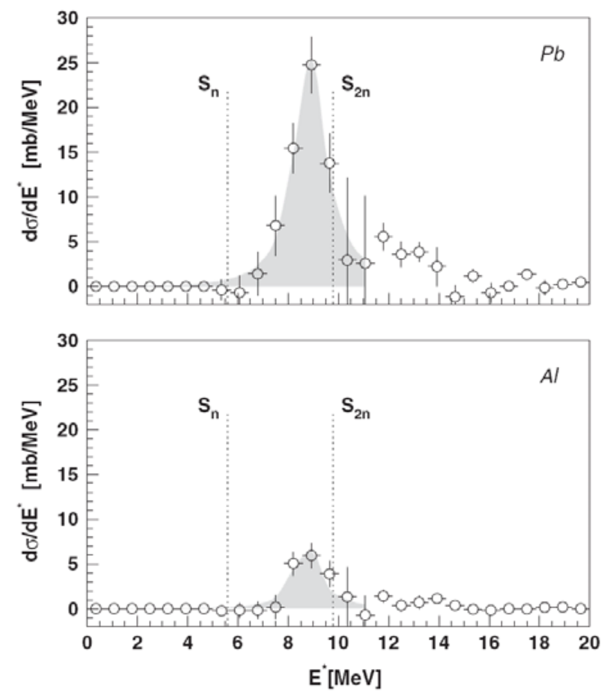

Formalism

$$H|\nu\rangle = E_\nu|\nu\rangle \qquad Q_\nu^\dagger|0\rangle = |\nu\rangle \qquad Q_\nu|0\rangle = 0$$

Particle-hole excitations RPA

$$Q_\nu^\dagger = \sum_{ph} X_{ph}^\nu a_p^\dagger a_h - Y_{ph}^\nu a_h^\dagger a_p$$

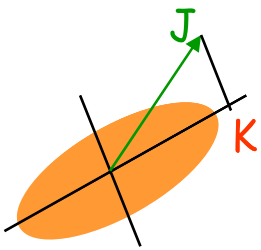

2-quasi-particles excitations QRPA

$$Q_\nu^+ = \sum_{ij} X_{ij}^\nu \eta_i^+ \eta_j^+ + Y_{ij}^\nu \eta_{\bar{j}} \eta_{\bar{i}}$$

$$\begin{pmatrix} A & B \\ B^* & A^* \end{pmatrix} \begin{pmatrix} X^\nu \\ Y^\nu \end{pmatrix} = \omega_\nu \begin{pmatrix} X^\nu \\ -Y^\nu \end{pmatrix}$$

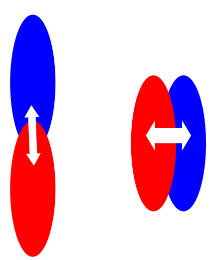

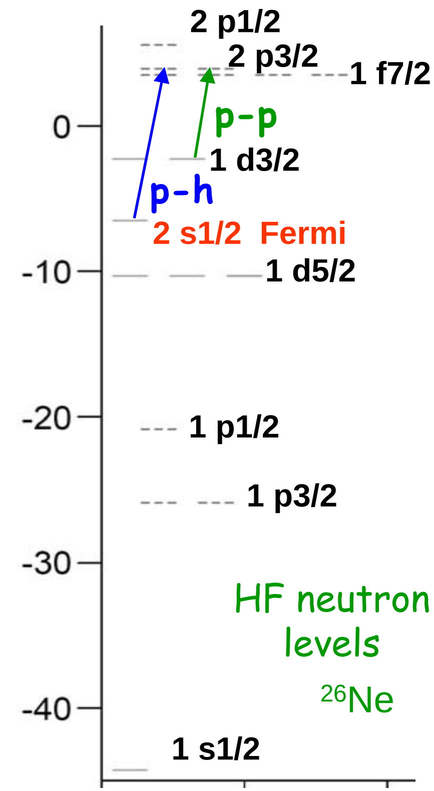

- Axially-symmetric-deformed nuclei
- Same (D1S Gogny) interaction in HFB and QRPA in order to avoid very dangerous inconsistencies

Other calculations by Bruyères-le-Châtel group

- ^{78}Ni, ^{100}Sn, ^{132}Sn, ^{208}Pb — *S. Péru, J.F. Berger, P.F. Bortignon EPJA 26, 25 (2005)*
- Si and Mg isotopes — *S. Péru, H. Goutte PRC 77,044313 (2008)*
- ^{238}U — *S. Péru, G. Gosselin, M. Martini, M. Dupuis, S. Hilaire, J.-C Devaux (2010)*

Typical example of dipole resonances study

energie atomique • energies alternatives

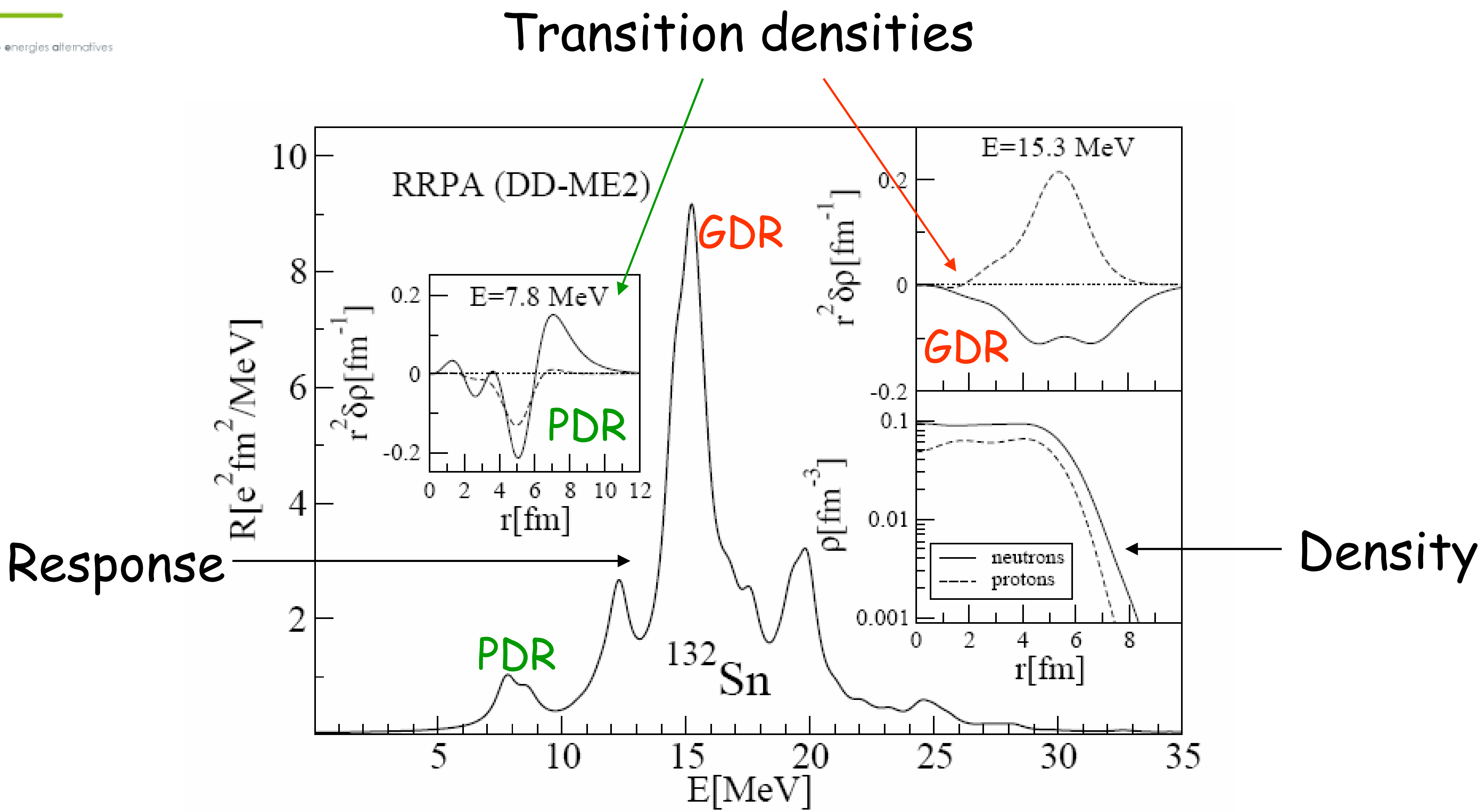

Paar et al. Rep. Prog. Phys. 70 (2007) 691-793

n and p densities through axially-deformed HFB

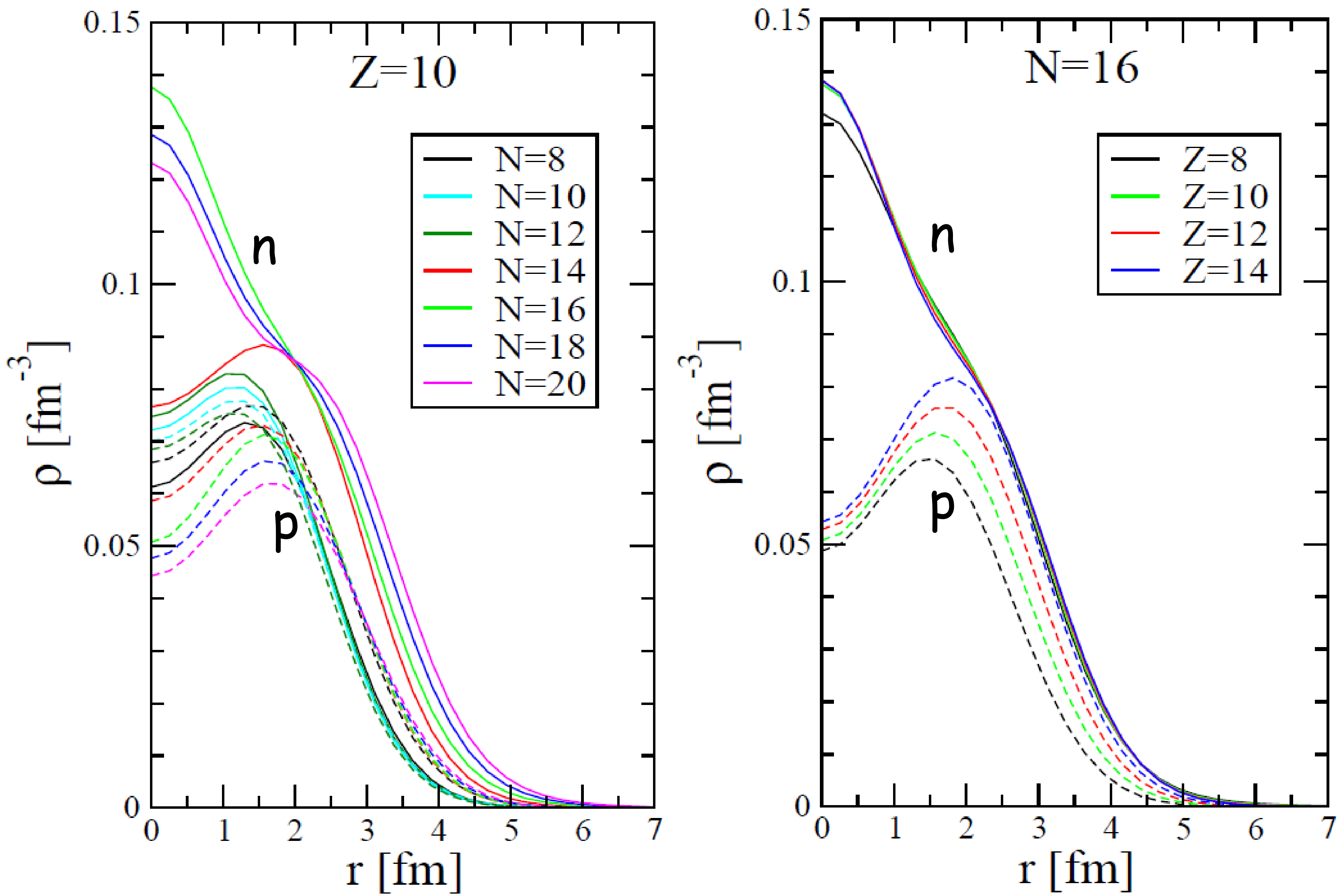

B(E1) QRPA distributions for Ne isotopes and N=16 isotones

Only 2 not spherical: prolate

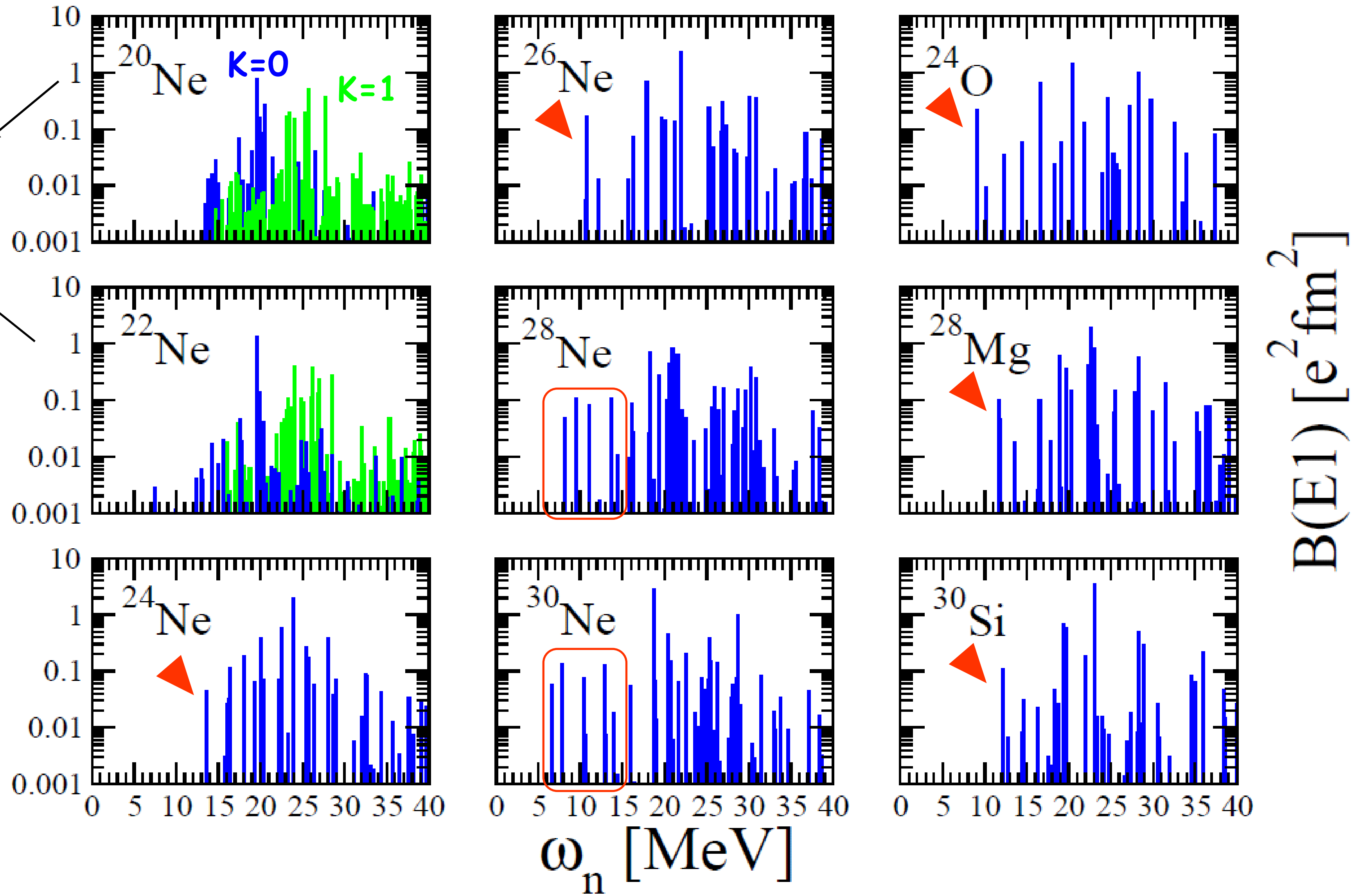

A dependence of low-lying excitations

energie atomique • energies alternatives

Neon isotopes

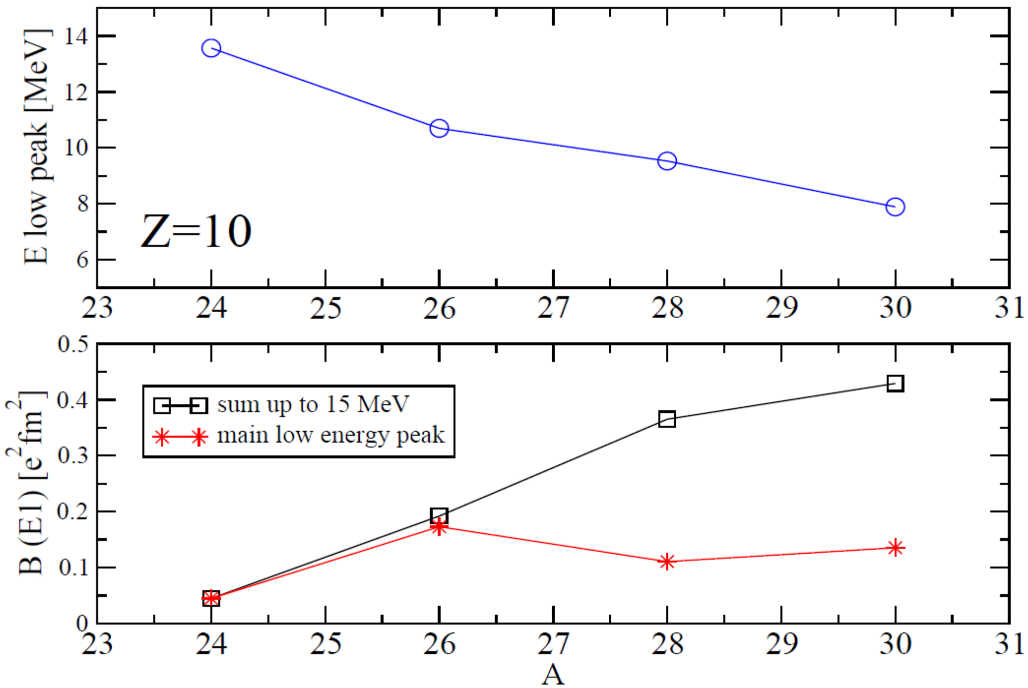

N=16 isotones

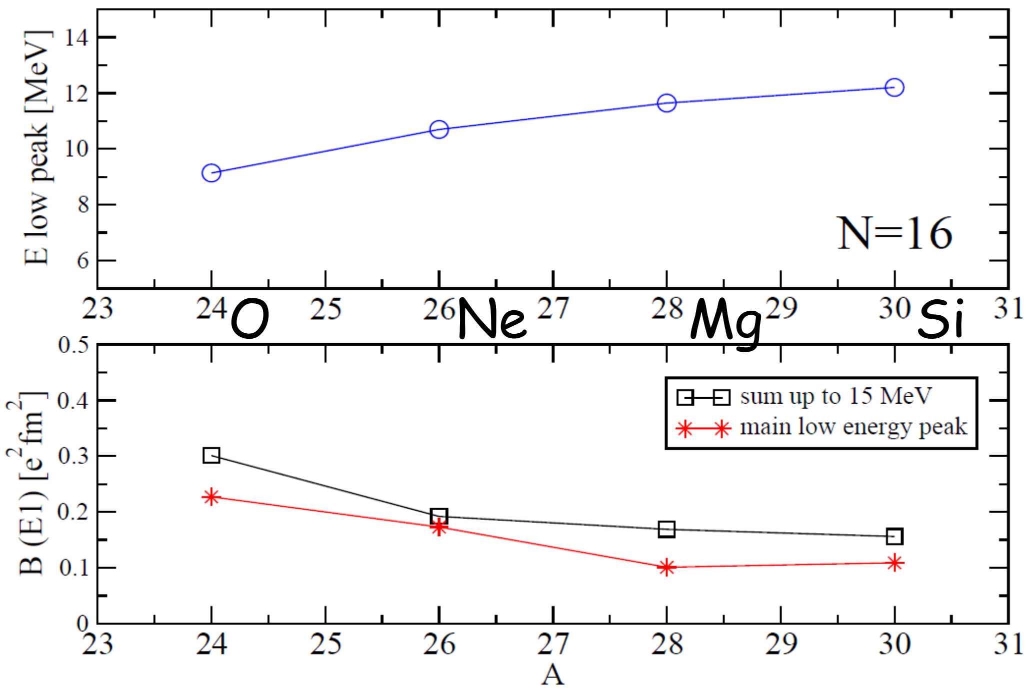

- The energy of the low peak decreases with the isospin asymmetry
- The B(E1) strength increases with the isospin asymmetry
- The fragmentation increases with the neutron number

energie atomique • energies alternatives

N=16 isotones

Main p-h (and p-p) configurations in N=16 isotones

	^{24}O	^{26}Ne	^{28}Mg	^{30}Si
first peak	9.1 MeV	10.7 MeV	11.6 MeV	12.2 MeV
ν $2s_{1/2}\rightarrow 2p_{3/2}$	73.5 % (8.92 MeV)	67.6 % (10.52 MeV)	39.7 % (11.68 MeV)	43.8 % (12.61 MeV)
ν $1d_{3/2}\rightarrow 2p_{3/2}$	0.0 % (9.26 MeV)	2.8 % (10.82 MeV)	32.7 % (11.93 MeV)	7.0 % (12.79 MeV)
ν $2s_{1/2}\rightarrow 2p_{1/2}$	10.0 % (10.33 MeV)	9.5 % (12.44 MeV)	5.8 % (13.98 MeV)	6.6 % (15.23 MeV)
ν $1d_{5/2}\rightarrow 1f_{7/2}$	8.7 % (12.87 MeV)	8.7 % (13.68 MeV)	8.2 % (14.18 MeV)	11.1 % (14.55 MeV)
ν $1d_{3/2}\rightarrow 2p_{1/2}$	0.0 % (10.67 MeV)	0.1 % (12.74 MeV)	2.7 % (14.22 MeV)	1.1 % (15.41 MeV)
ν $1p_{1/2}\rightarrow 1d_{3/2}$	1.2 % (17.70 MeV)	1.1 % (18.50 MeV)	0.5 % (19.10 MeV)	0.3 % (19.60 MeV)
ν total contribution	94.6 %	91.9 %	90.6 %	70.9 %
π $1p_{1/2}\rightarrow 2s_{1/2}$	2.0 % (15.19 MeV)	4.1 % (15.97 MeV)	5.6 % (16.22 MeV)	18.5 % (15.92 MeV)
π $p_{3/2}$ $1d_{5/2}$	2.7 % (15.89 MeV)	2.0 % (17.60 MeV)	0.8 % (18.97 MeV)	0.9 % (17.15 MeV)
	($1p_{3/2}\rightarrow$ $1d_{5/2}$)	($1p_{3/2}\rightarrow$ $1d_{5/2}$)	($1p_{3/2}\rightarrow$ $1d_{5/2}$)	($1d_{5/2}\rightarrow 2p_{3/2}$)
π $1d_{5/2}\rightarrow 1f_{7/2}$	0.0 % (24.80 MeV)	0.9 % (17.48 MeV)	1.9 % (16.02 MeV)	7.7 % (14.33 MeV)
π total contribution	5.4 %	8.1 %	9.4 %	29.1 %
main peak (GDR)	20.5 MeV	21.9 MeV	22.6 MeV	23.1 MeV
ν total contribution	80.5 %	64.5 %	78.5 %	54.4 %
π total contribution	19.5. %	35.5 %	21.5 %	45.6 %
N/A	66.7 %	61.5 %	57.1 %	53.3 %

Introduction of indexes in order to measure the collectivity

Let's $N_{2\mathrm{qp}}$ the number of all the possible 2-qp excitations for a given K

$N_{2\mathrm{qp}}$ = 4832 in our case

Well known normalization of the QRPA amplitude: $$\sum_{2\mathrm{qp}=1}^{N_{2\mathrm{qp}}} [(X^n_{2\mathrm{qp}})^2 - (Y^n_{2\mathrm{qp}})^2] = 1$$

We introduce the number of states with $$[(X^n_{2\mathrm{qp}})^2 - (Y^n_{2\mathrm{qp}})^2] \geq \frac{1}{N_{2\mathrm{qp}}}$$

$N^\star_\nu$ Neutron contribution

$N^\star_\pi$ Proton contribution

Ideal collective case:
all the 2-qp excitations contribute $$N^\star = N^\star_\nu + N^\star_\pi = N_{2\mathrm{qp}}$$

Excitation produced by a single 2-qp state: $N^\star = 1$

Values of collectivity indexes in the N=16 isotones

energie atomique • energies alternatives

	ω (MeV)	$N^\star_\nu$	$N^\star_\pi$	ν tot.	π tot.
	^{24}**O**				
	9.1	34	10	94.6 %	5.4 %
GDR	20.5	62	12	80.5 %	19.5 %
	^{26}**Ne**				
	10.7	30	18	91.9 %	8.1 %
GDR	21.9	56	26	64.5 %	35.5 %
	^{28}**Mg**				
	11.6	24	22	90.6 %	9.4 %
GDR	22.6	82	32	78.5 %	21.5 %
	^{30}**Si**				
	12.2	32	22	70.9 %	29.1 %
GDR	23.1	54	34	54.4 %	45.6 %

$N^\star$ lightly increases from ^{24}O to ^{30}Si

$N^\star_\nu$ decreases with Z

$N^\star_\pi$ increases with Z

$N^\star$ of low energy peak is ~ 60% of GDR

Neutron and proton transition densities

Low energy

center: isovector

surface: isoscalar

GDR isovector n and p in opposite phase

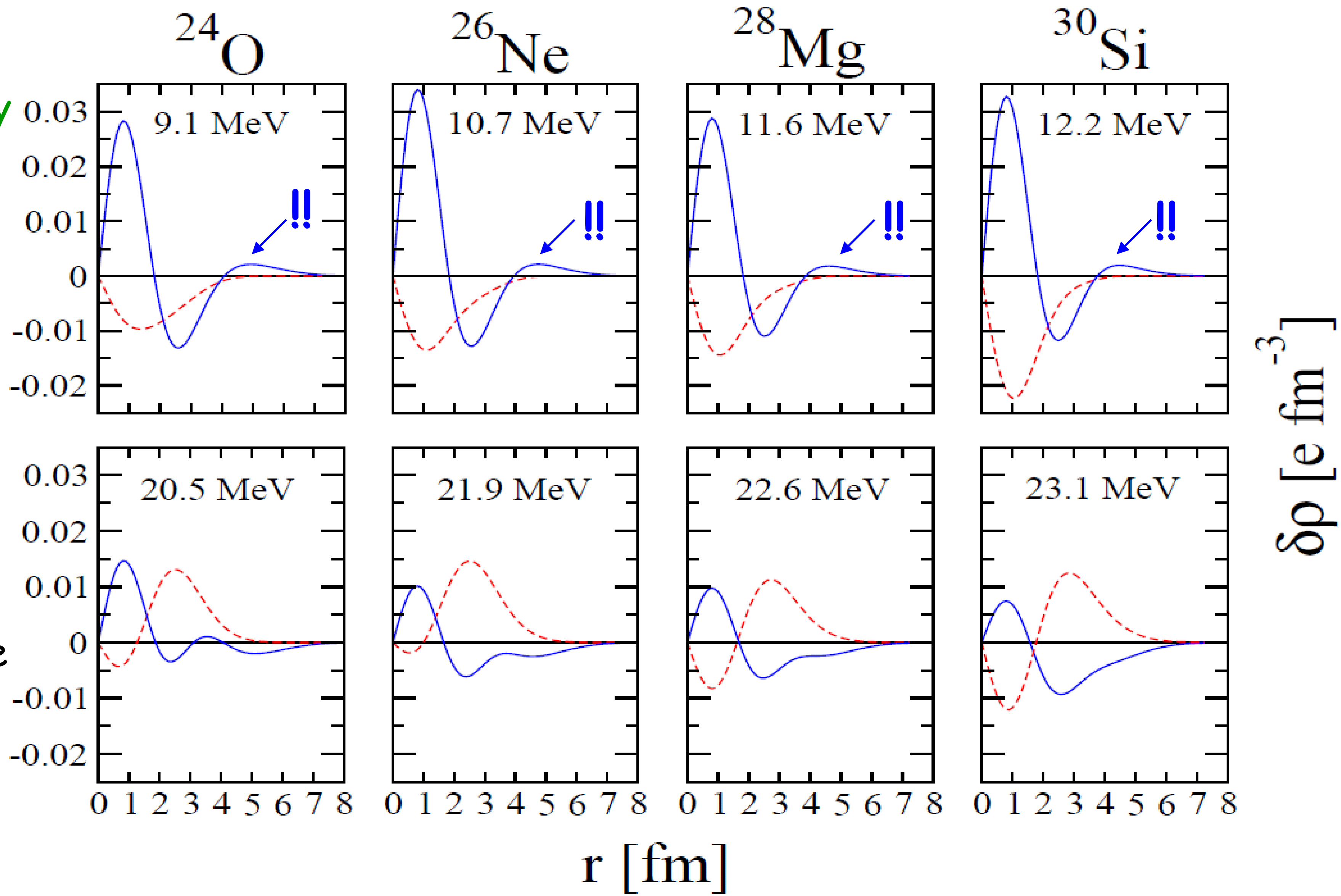

energie atomique • energies alternatives

Summary of low-lying dipole excitations in N=16 isotones

Similar behavior in ^{24}O, ^{26}Ne, ^{28}Mg, ^{30}Si

- Small but finite collectivity
- Non trivial transition densities
due to spatially extended structure of 2s1/2 neutron state

⇒ Some interesting low energy properties can be obtained also from the stable ^{28}Mg and ^{30}Si nuclei

Neon isotopes

B(E1) QRPA distributions for Neon isotopes

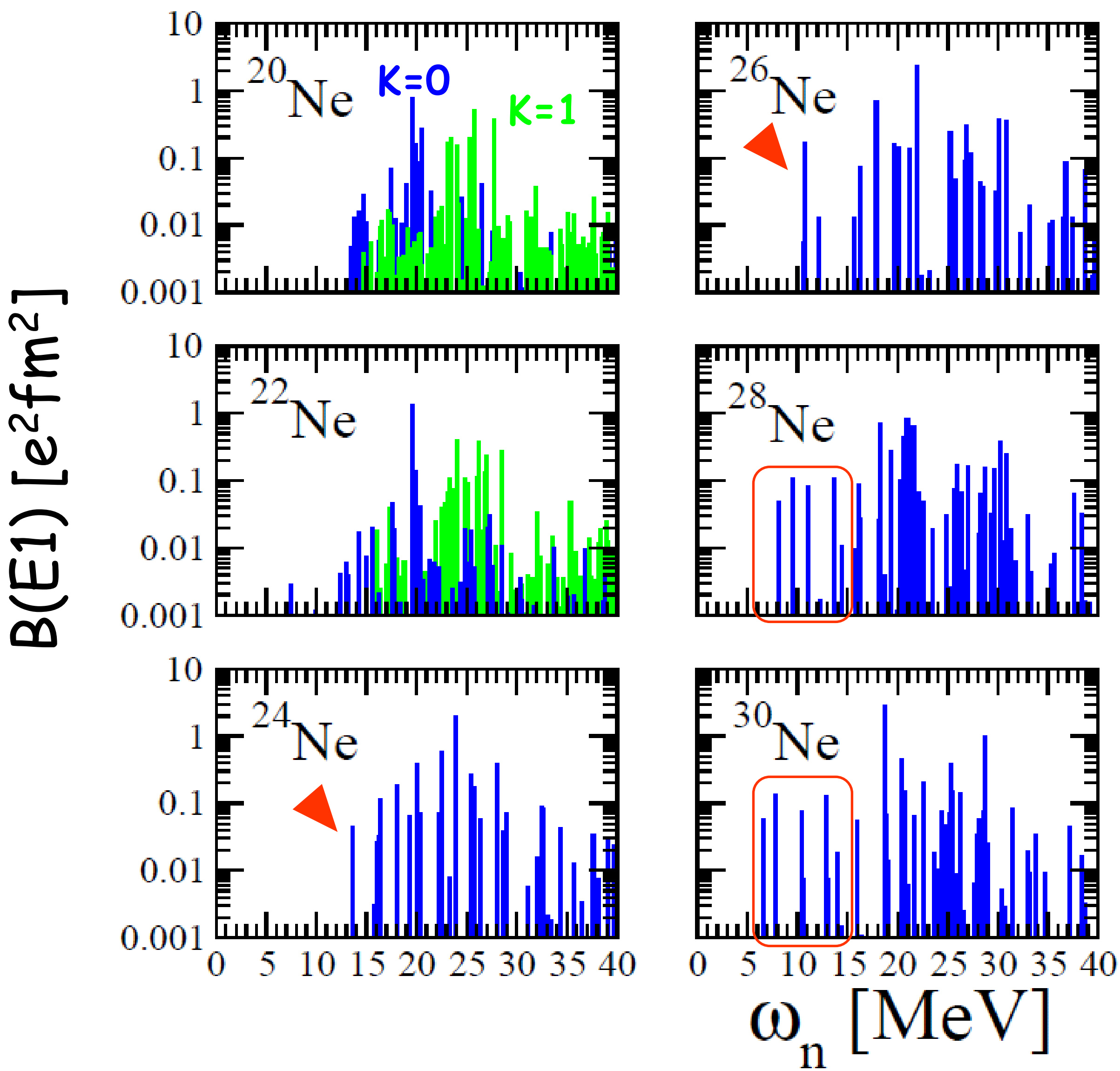

Values of collectivity indexes in the Neon isotopes

ω (MeV)	$N_\nu^\star$	$N_\pi^\star$	ν tot.	π tot.	
^{24}**Ne**					
13.6	44	8	97.7 %	2.3 %	
16.4	32	16	55.1 %	44.9 %	
23.9	60	24	65.0 %	35.0 %	GDR
^{26}**Ne**					
10.7	30	18	91.9 %	8.1 %	
21.9	56	26	65.5 %	35.5 %	GDR

ω (MeV)	$N_\nu^\star$	$N_\pi^\star$	ν tot.	π tot.	
^{28}**Ne**					
8.1	24	12	98.7 %	1.3 %	
9.5	26	14	98.4 %	1.6 %	
11.1	30	16	95.2 %	4.8 %	
13.7	72	14	97.1 %	2.9 %	
16.1	32	46	5.0 %	95.0 %	
18.3	76	26	91.5 %	8.5 %	
20.9	92	32	70.2 %	29.8 %	GDR
^{30}**Ne**					
6.6	18	10	98.9 %	1.1 %	
7.9	20	14	98.9 %	1.1 %	
10.5	40	16	96.9 %	3.1 %	
12.8	64	16	97.0 %	3.0 %	
16.0	26	42	3.2 %	96.8 %	
18.7	98	44	68.3 %	31.7 %	GDR

^{24}Ne

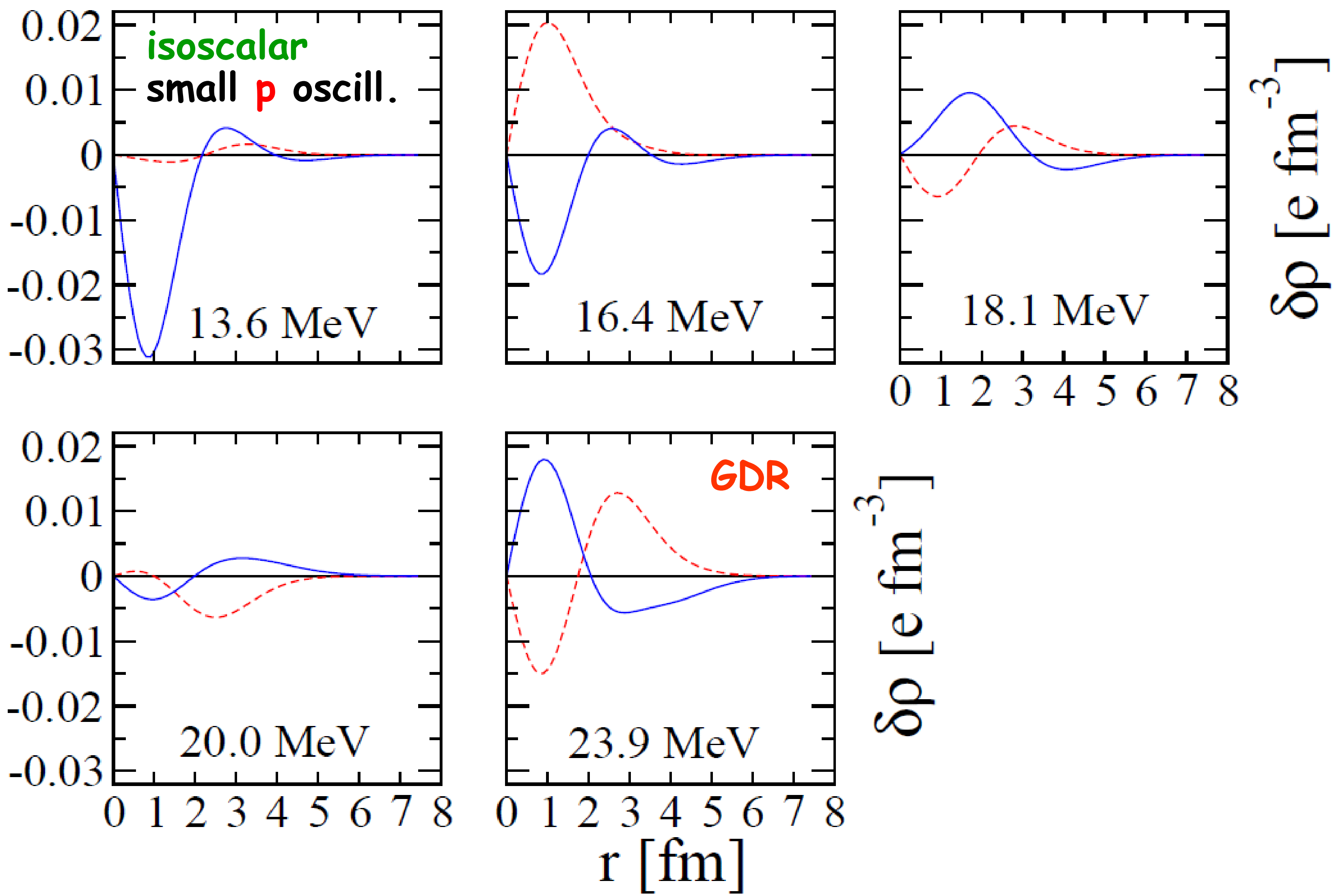

isoscalar
small p oscill.
13.6 MeV
16.4 MeV
18.1 MeV
20.0 MeV
GDR
23.9 MeV
0.02
0.01
0
-0.01
-0.02
-0.03
0 1 2 3 4 5 6 7 8
r [fm]
δρ [e fm^{-3}]

^{28}Ne

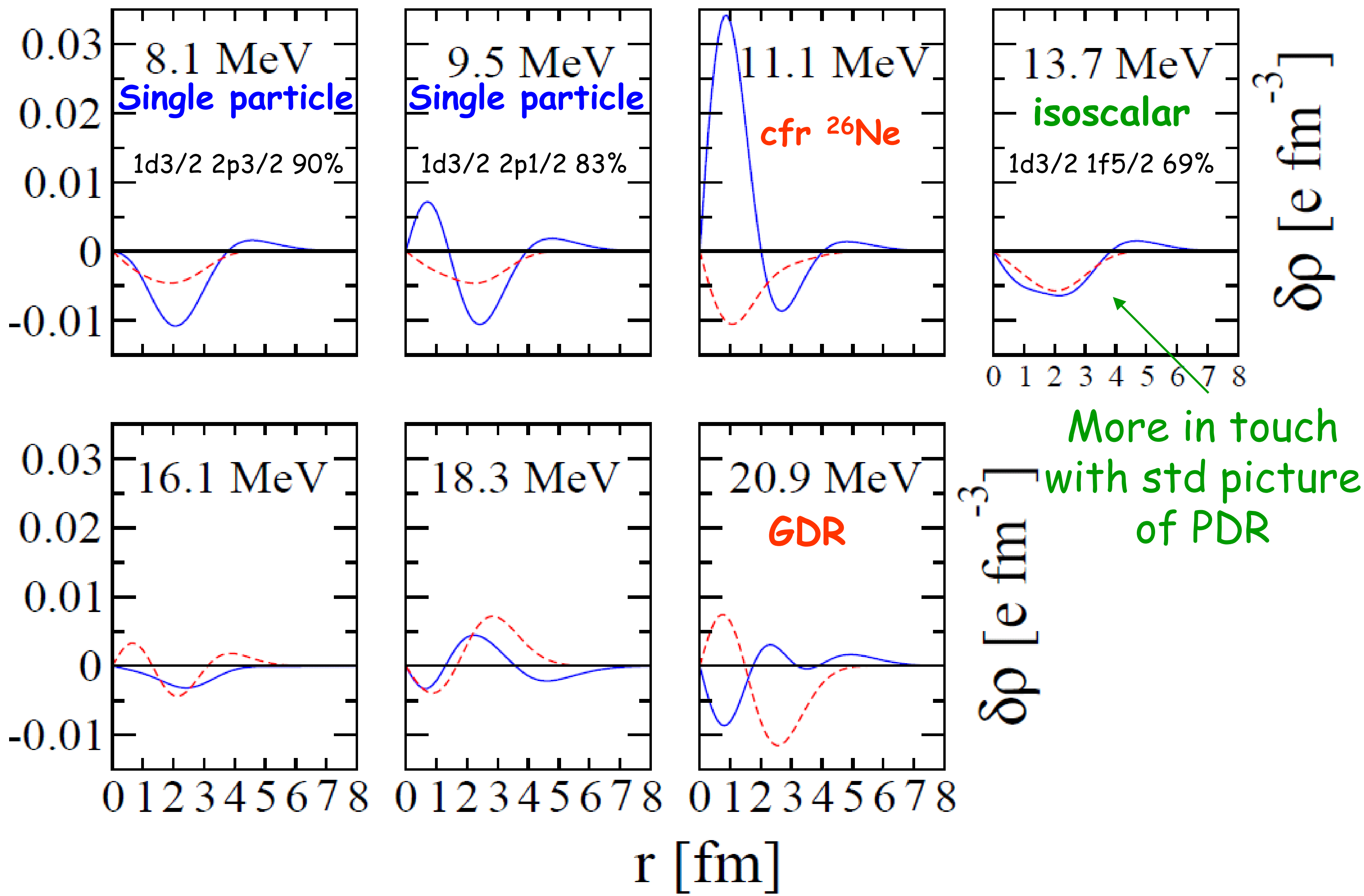

8.1 MeV
Single particle
1d3/2 2p3/2 90%
9.5 MeV
Single particle
1d3/2 2p1/2 83%
11.1 MeV
cfr 26Ne
13.7 MeV
isoscalar
1d3/2 1f5/2 69%
16.1 MeV
18.3 MeV
20.9 MeV
GDR
0.03
0.02
0.01
0
-0.01
0 1 2 3 4 5 6 7 8
δρ [e fm-3]
r [fm]
More in touch with std picture of PDR

^{30}Ne

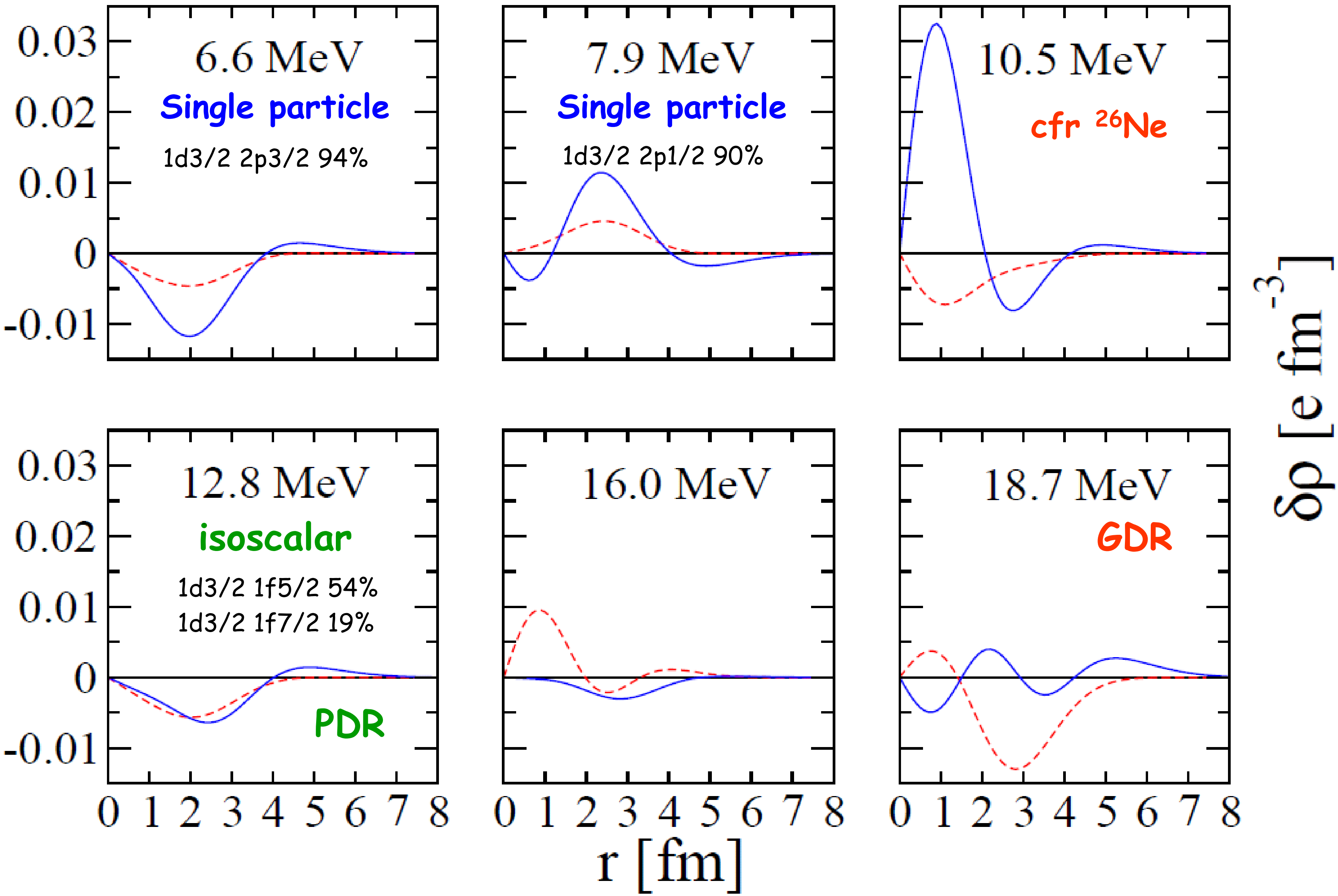
0.03
0.02
0.01
0
-0.01
6.6 MeV
Single particle
1d3/2 2p3/2 94%
7.9 MeV
Single particle
1d3/2 2p1/2 90%
10.5 MeV
cfr 26Ne
12.8 MeV
isoscalar
1d3/2 1f5/2 54%
1d3/2 1f7/2 19%
PDR
16.0 MeV
18.7 MeV
GDR
0 1 2 3 4 5 6 7 8
r [fm]
δρ [e fm-3]

Summary of low-lying dipole excitations in Neon isotopes

- The strength of the low-energy state increases with N
- Increasing N the strength distribution is more fragmented
- Appearance of a collective state in ^{28}Ne and ^{30}Ne
- Isoscalar behavior of the transition densities of this state
- Picture more in touch with the standard behavior of PDR

energie atomique • energies alternatives

Proton PDR in ^{18}Ne

energie atomique • energies alternatives

^{18}Ne

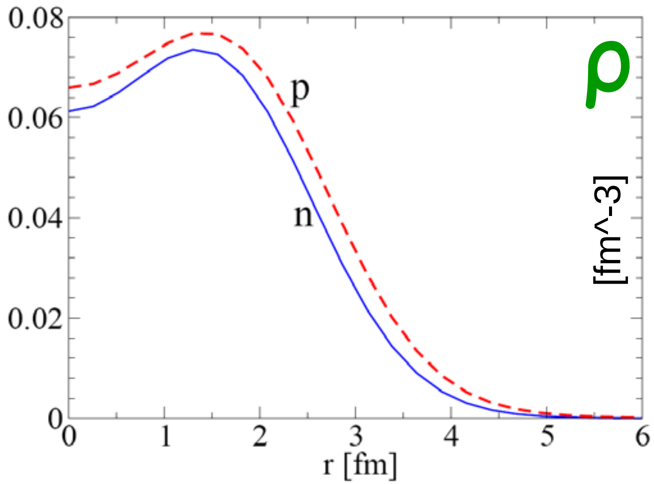

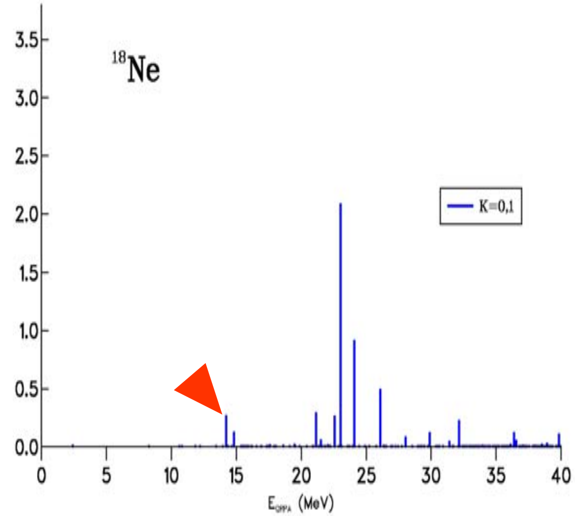

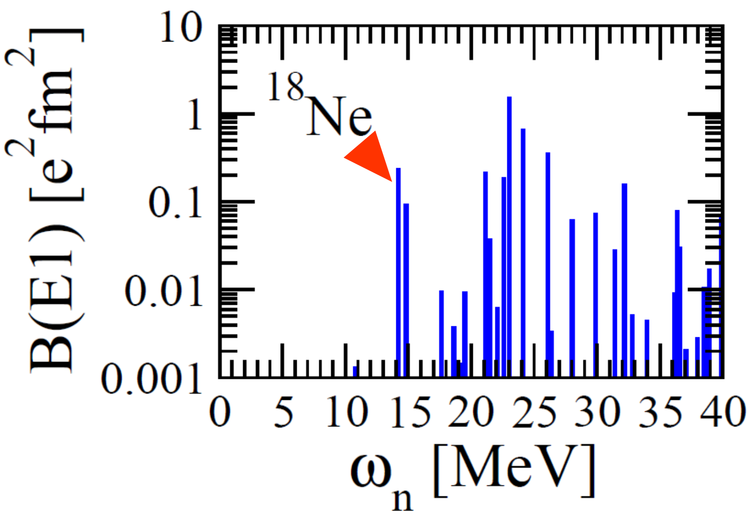

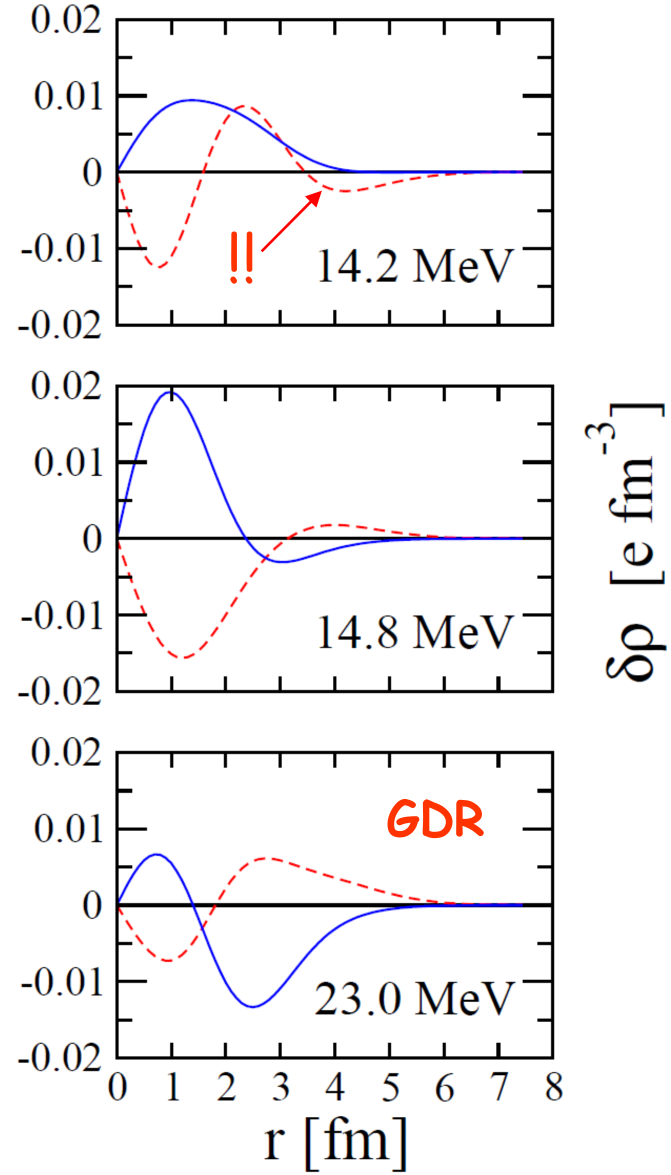

Microscopical analysis of ^{18}Ne dipole excitations

	first low energy peak 14.2 MeV	second low energy peak 14.8 MeV
π $1d_{5/2} \rightarrow 1f_{7/2}$ (15.99 MeV)	29.1 %	1.6 %
π $1d_{5/2} \rightarrow 2p_{3/2}$ (15.98 MeV)	23.2 %	6.3 %
π $1p_{1/2} \rightarrow 2s_{1/2}$ (13.75 MeV)	11.7 %	35.2 %
π $2s_{1/2} \rightarrow 2p_{3/2}$ (18.19 MeV)	9.3 %	1.2%
π $1p_{3/2} \rightarrow 1d_{5/2}$ (16.95 MeV)	8.5 %	9.3 %
π $2s_{1/2} \rightarrow 2p_{3/2}$ (19.14 MeV)	2.7 %	0.5%
π total contribution	92.2 %	55.7 %
ν $1p_{3/2} \rightarrow 1d_{3/2}$ (15.78 MeV)	3.8 %	2.7 %
ν $1p_{1/2} \rightarrow 2s_{1/2}$ (14.18 MeV)	3.6 %	41.0 %
ν total contribution	7.8 %	44.3 %

	ω (MeV)	$N_\nu^\star$	$N_\pi^\star$	ν tot.	π tot.
	^{18}Ne				
	14.2	12	60	7.8 %	92.2 %
	14.8	10	36	44.3 %	55.7 %
GDR	23.0	16	56	21.9 %	78.1 %

Dominant role of protons in the 1^ state

Collectivity of 1^ state the same as GDR

⬇

Proton PDR in ^{18}Ne

Summary

Low energy dipole excitations in axially-symmetric deformed HFB+QRPA

N=16 isotones

- Similar behavior in ^{24}O, ^{26}Ne, ^{28}Mg, ^{30}Si
- Small but finite collectivity; non-trivial transition densities

Neon isotopes

- Increase of low-energy strength and fragmentation with N
- Appearance of a collective isoscalar state in ^{28}Ne and ^{30}Ne

^{18}Ne

- Appearance of a proton PDR

Perspectives

- Detailed analysis of PDR in exotic nuclei of experimental interest
- Large-scale QRPA calculations of E1 strength and (n,γ) reactions (massive parallel computation of ^{238}U responses recently performed)

Spares

Identification of the spurious state

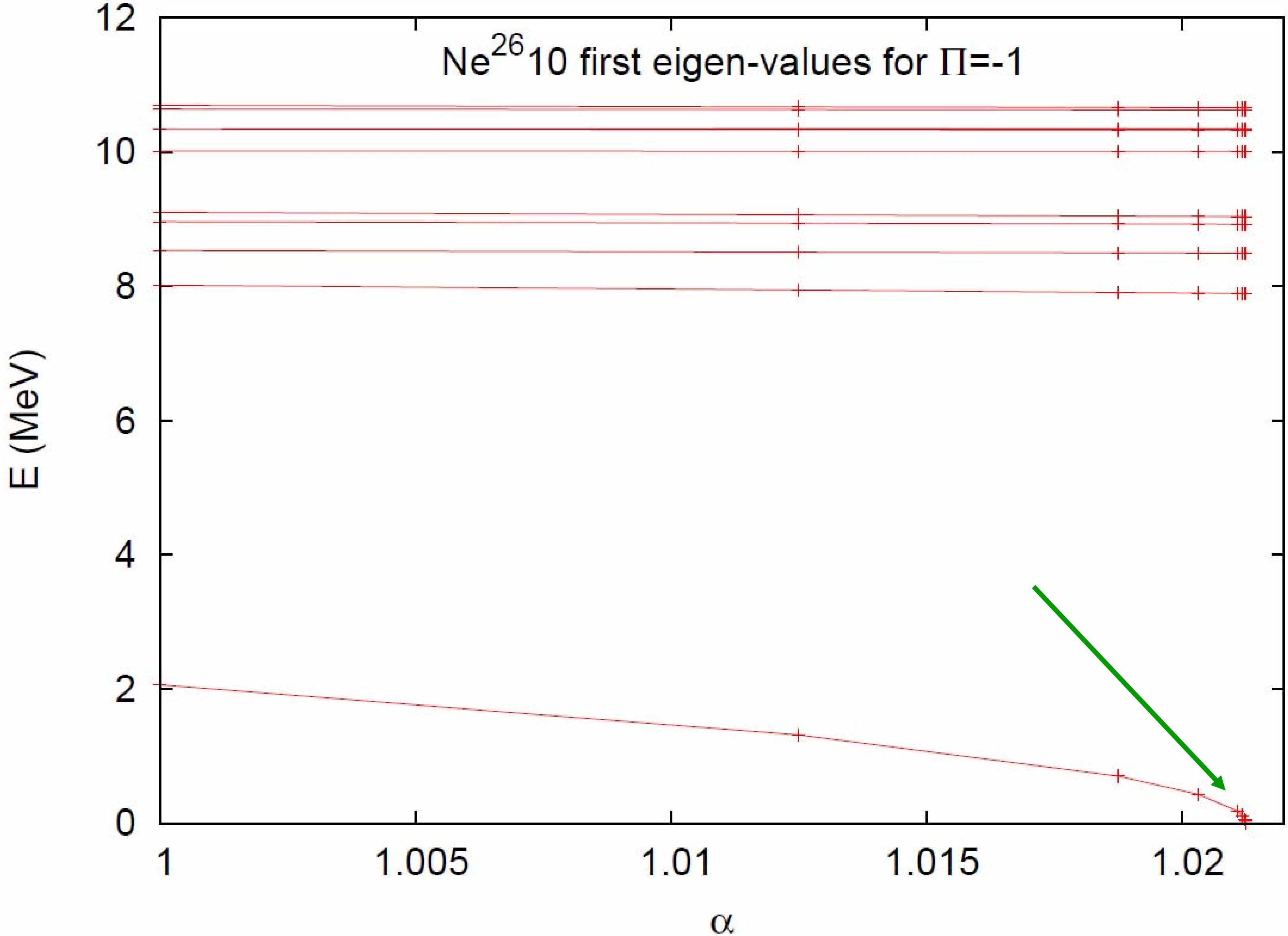

Identification of the spurious state

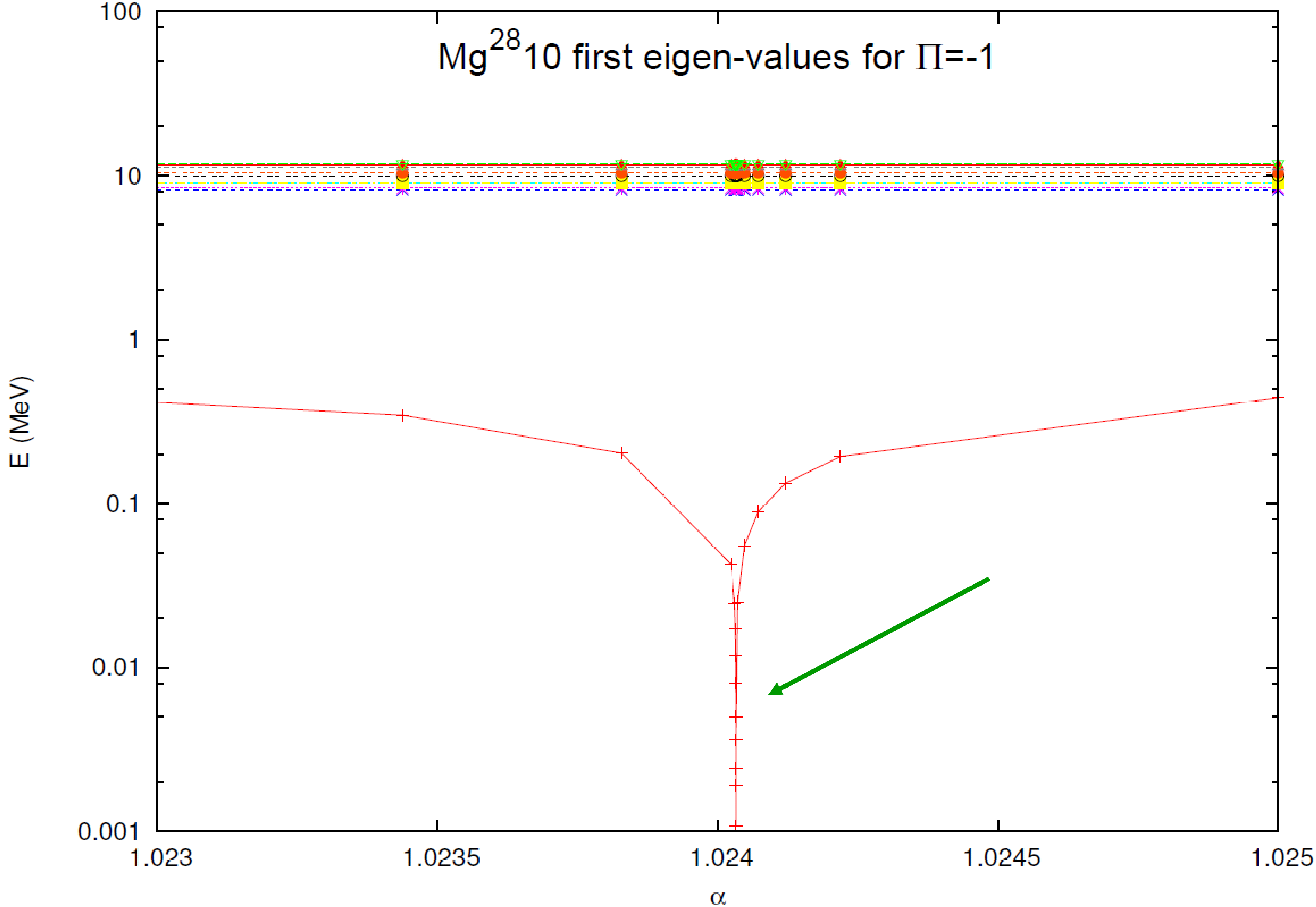

Hartree-Fock (-Bogoliubov)

energie atomique • energies alternatives

HF

$$|\psi_{HF}\rangle = \left(\prod_{i=1}^{A} a_i^+\right)|0\rangle \qquad H = \sum_{l_1 l_2} t_{l_1 l_2} c_{l_1}^+ c_{l_2} + \frac{1}{4}\sum_{l_1 l_2 l_3 l_4} \bar{v}_{l_1 l_2, l_3 l_4} c_{l_1}^+ c_{l_2}^+ c_{l_4} c_{l_3}$$

$$a_p|\psi_{HF}\rangle = 0 \qquad a_\alpha^+ = \sum U_{i\alpha} C_i^+ \qquad \phi_\alpha = \sum U_{i\alpha}\chi_i \qquad \rho_{ij} = \langle\psi_{HF}|C_j^+ C_i|\psi_{HF}\rangle = \sum_{\alpha=1}^{A} U_{i\alpha} U_{j\alpha}^\star$$

$$a_i^+|\psi_{HF}\rangle = 0 \qquad \mathcal{E}(\psi_{HF}) = \mathcal{E}(\rho) = \mathrm{Tr}(t\rho) + \frac{1}{2}\mathrm{Tr}_1\mathrm{Tr}_2(\rho_1 \bar{v}_{12}\rho_2)$$

$$[h,\rho] = 0 \qquad h = \frac{\partial\mathcal{E}(\rho)}{\partial\rho} \qquad \sum_{l'} h_{ll'} U_{l'k} = \sum_{l'}\left(t_{ll'} + \sum_{i=1}^{A}\sum_{pp'} \bar{v}_{lp'l'p} U_{pi} U_{p'i}^\star\right) U_{l'k} = \epsilon_k U_{lk}$$

HFB

$$|\psi_{HFB}\rangle = \left(\prod_{\nu}\eta_\nu\right)|0\rangle \qquad \rho_{ij} = \langle\psi_{HFB}|C_j^+ C_i|\psi_{HFB}\rangle \qquad k_{ij} = \langle\psi_{HFB}|C_i C_j|\psi_{HFB}\rangle$$

$$\eta_\nu|\psi_{HFB}\rangle = 0 \qquad \mathcal{E}(\psi_{HFB}) = \mathcal{E}(\rho k) = \mathrm{Tr}(t\rho) + \frac{1}{2}\mathrm{Tr}_1\mathrm{Tr}_2(\rho_1\bar{v}_{12}\rho_2) + \frac{1}{4}\sum_{\alpha\beta\gamma\delta} v_{\alpha\beta\gamma\delta} k_{\beta\alpha}^\star k_{\delta\gamma}$$

$$\begin{pmatrix}\eta\\ \eta^+\end{pmatrix} = B\begin{pmatrix}C\\ C^+\end{pmatrix} = \begin{pmatrix}U & V\\ V^* & U^*\end{pmatrix}\begin{pmatrix}C\\ C^+\end{pmatrix} \qquad H_B = \begin{pmatrix}e & \Delta\\ \tilde{\Delta} & -e\end{pmatrix} \qquad e = \frac{\partial\mathcal{E}(\rho k)}{\partial\rho} \qquad \Delta = \frac{\partial\mathcal{E}(\rho k)}{\partial k} \qquad H_B\tilde{B} = E\tilde{B}$$

$^{18}_{10}Ne_{8}$

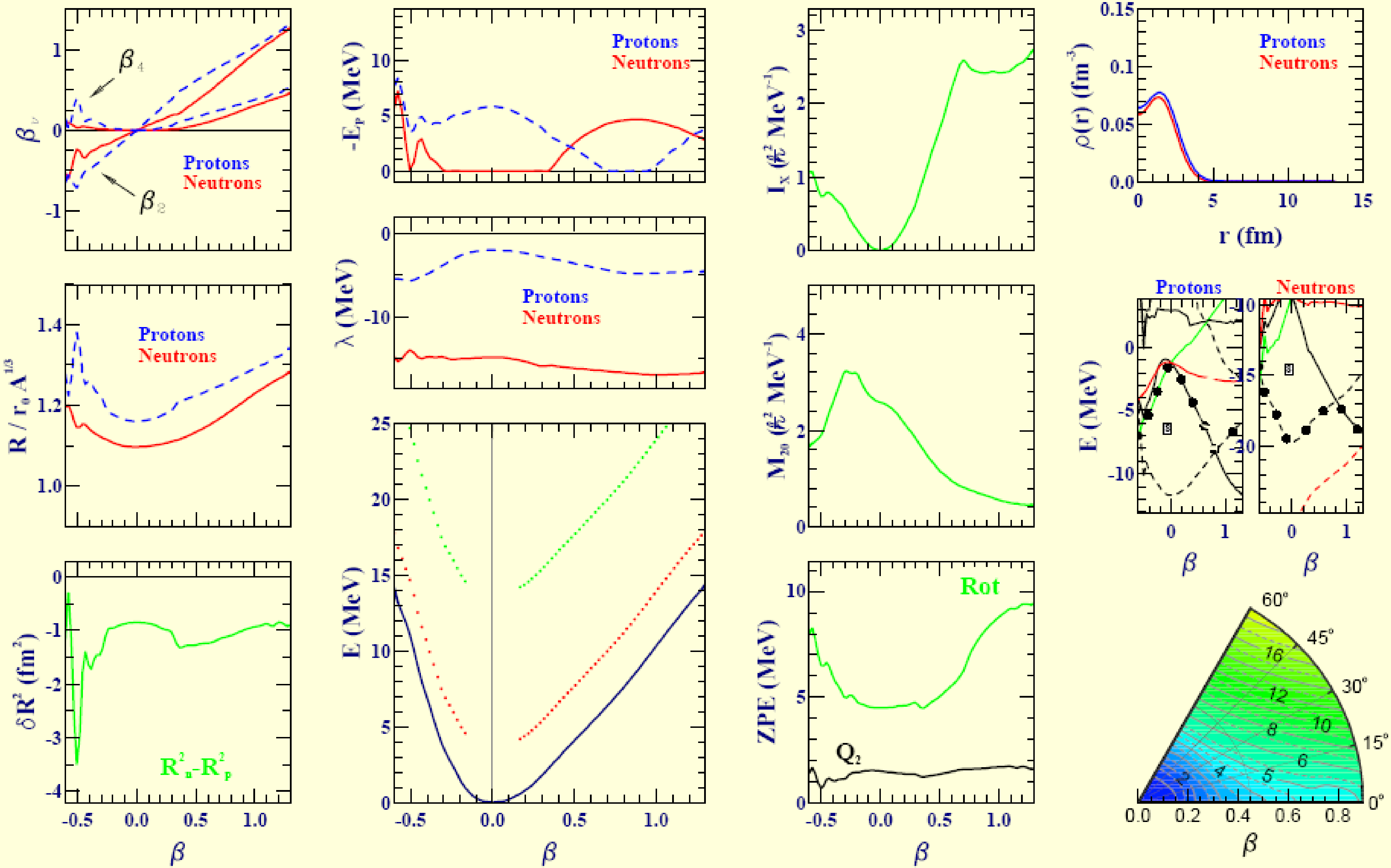

HFB-D1S Bruyères-le-Châtel

$^{20}_{10}\mathrm{Ne}_{10}$

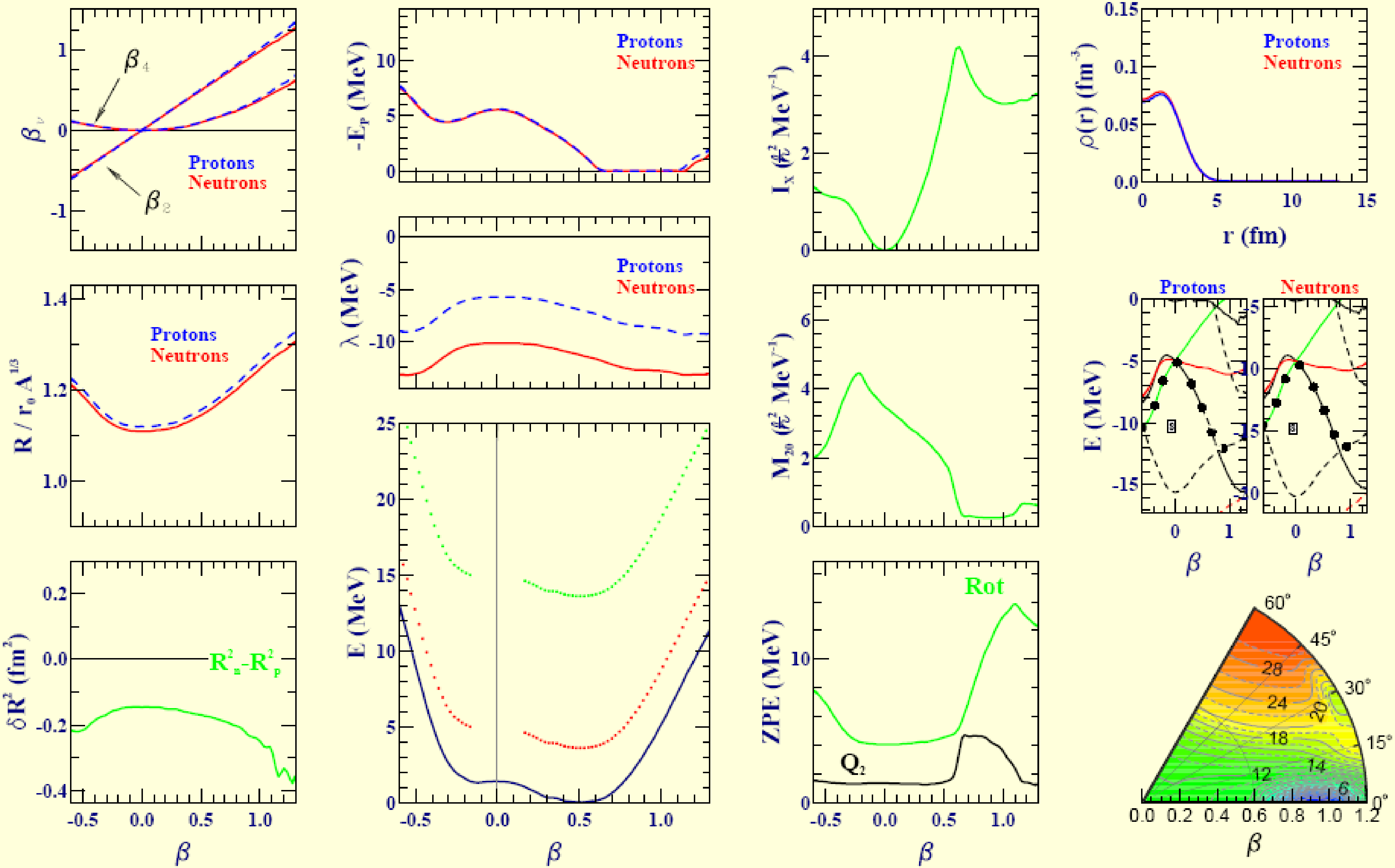

HFB-D1S Bruyères-le-Châtel

$^{22}_{10}Ne_{12}$

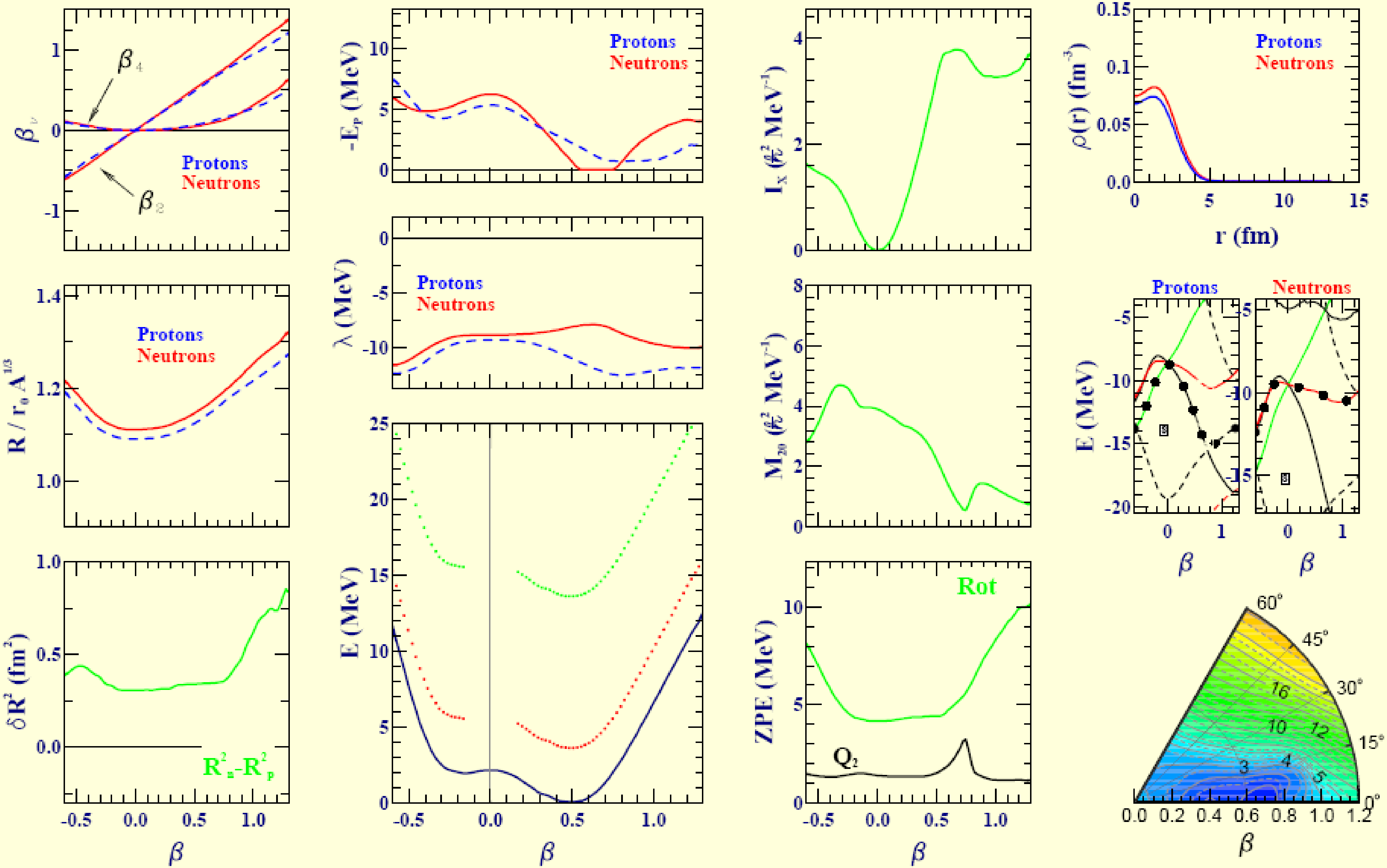

HFB-D1S Bruyères-le-Châtel

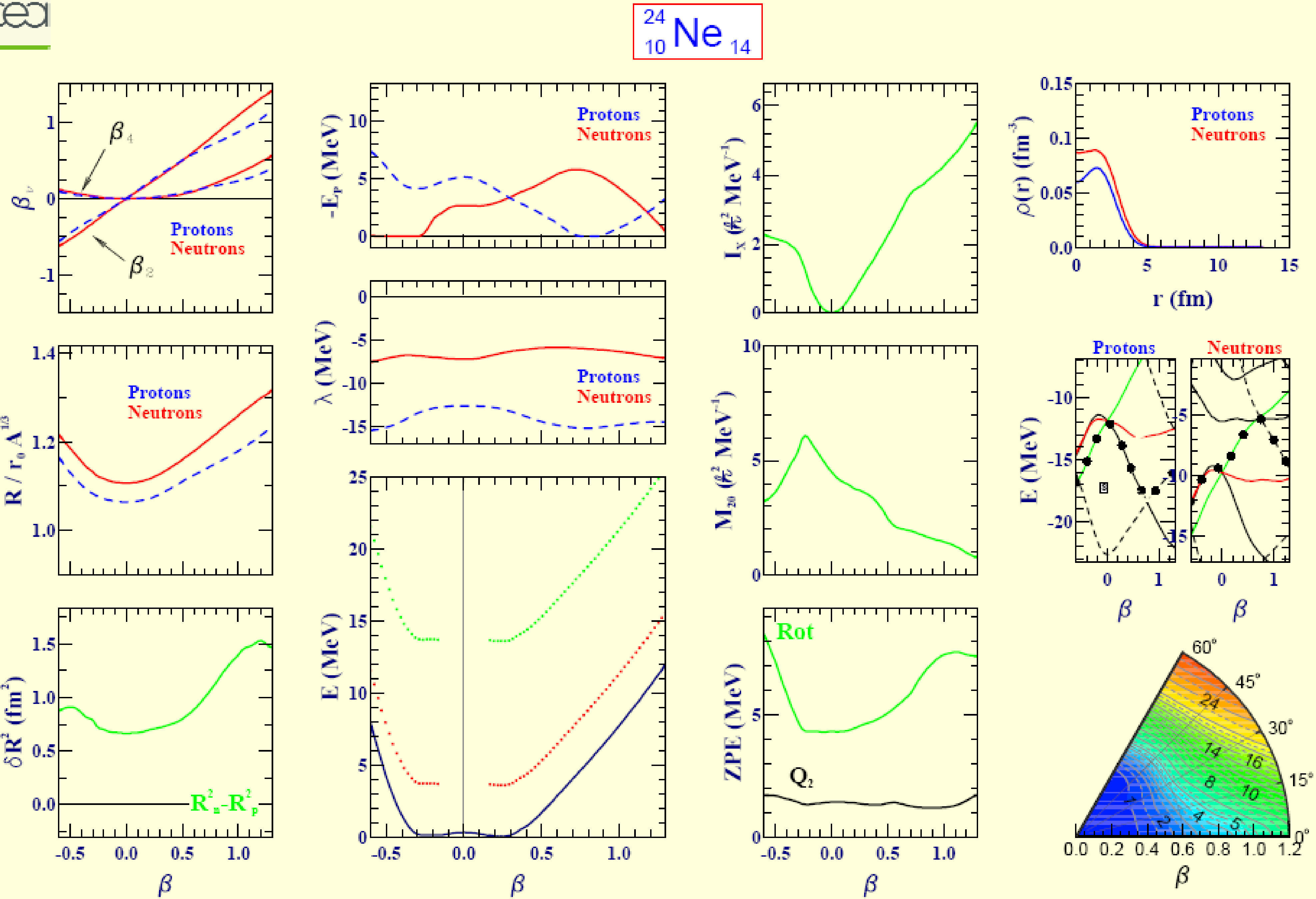

HFB-D1S Bruyères-le-Châtel

$^{26}_{10}\text{Ne}_{16}$

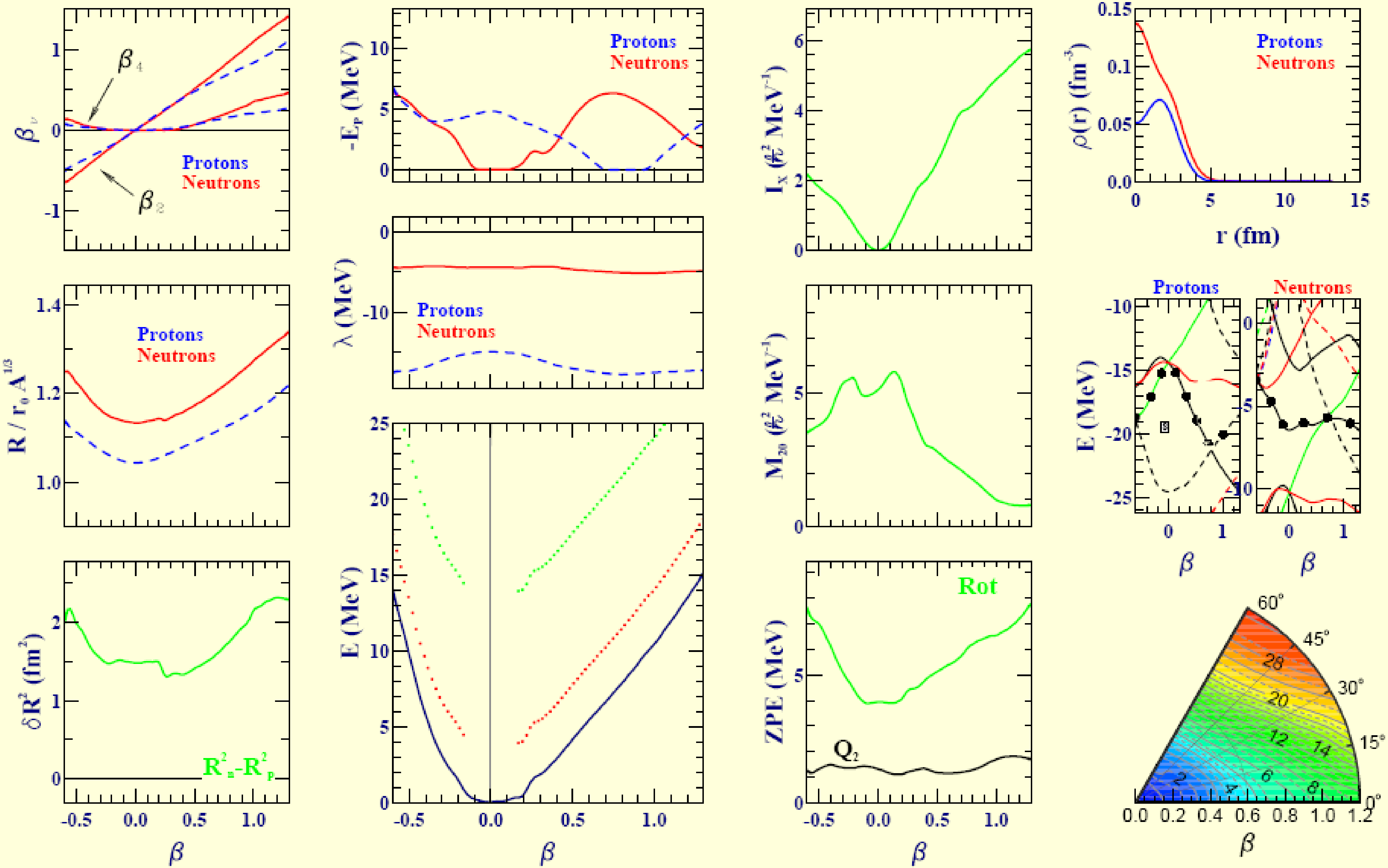

HFB-D1S Bruyères-le-Châtel

$^{28}_{10}Ne_{18}$

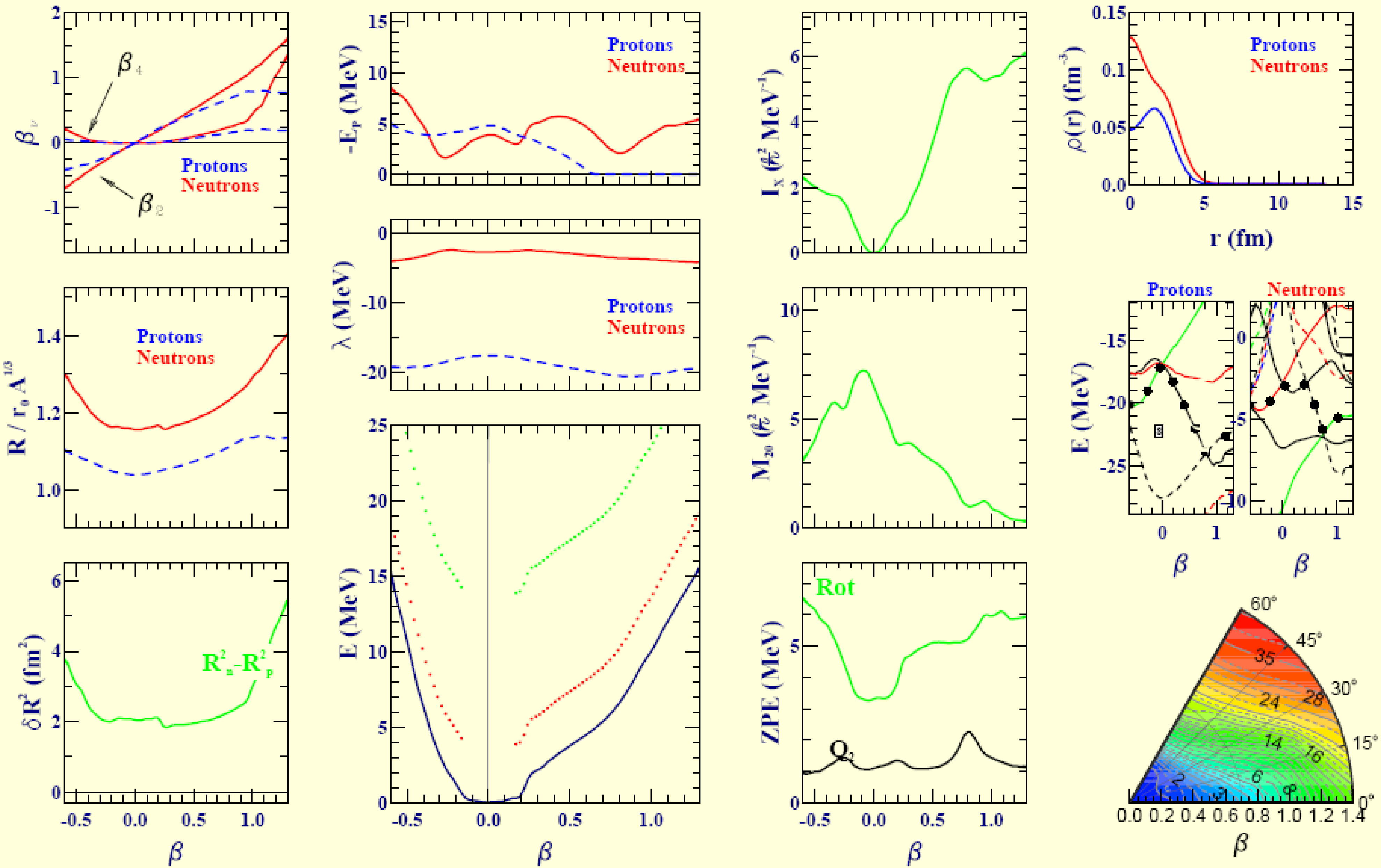

HFB-D1S Bruyères-le-Châtel

$^{30}_{10}Ne_{20}$

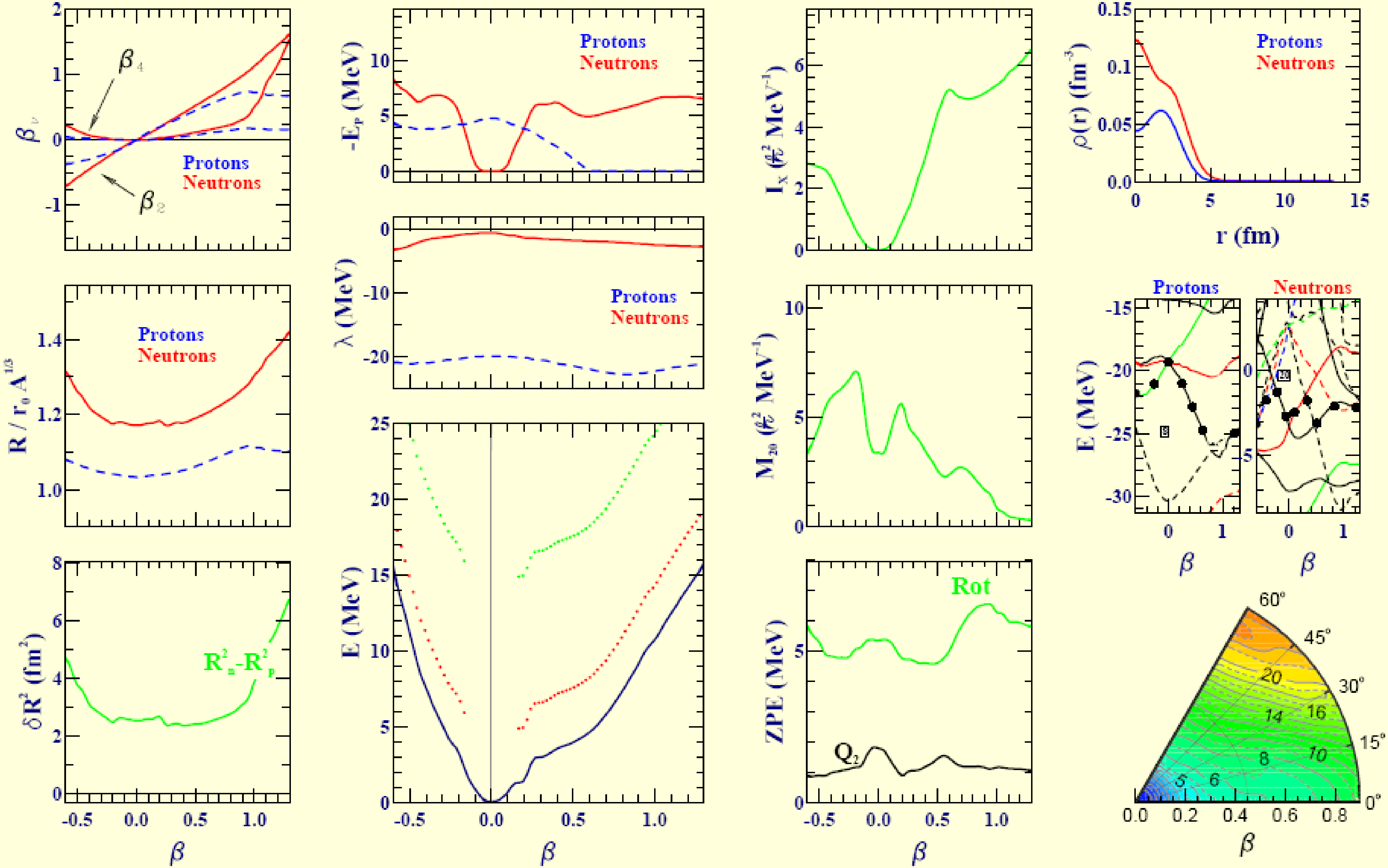

Protons
Neutrons
β_4
β_2
β_ν
$-E_p$ (MeV)
I_x ($\hbar^2$ MeV^{-1})
$\rho(r)$ (fm^{-3})
r (fm)
R / r_0 A$^{1/3}$
λ (MeV)
M_{20} ($\hbar^2$ MeV^{-1})
E (MeV)
δR^2 (fm^2)
R^2_n-R^2_p
ZPE (MeV)
Rot
Q_2
β
60°
45°
30°
15°
0°

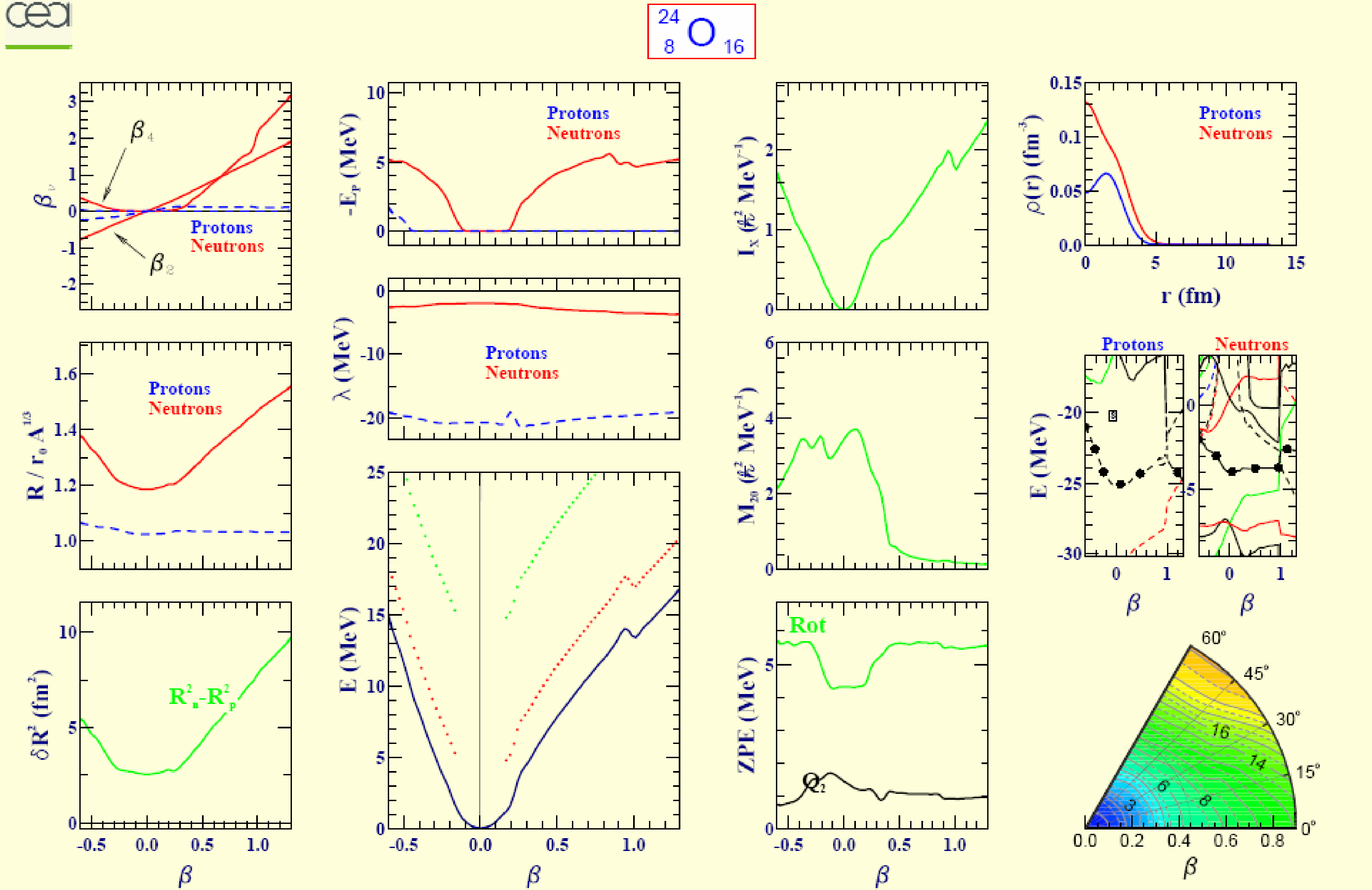

HFB-D1S Bruyères-le-Châtel

$^{28}_{12}Mg_{16}$

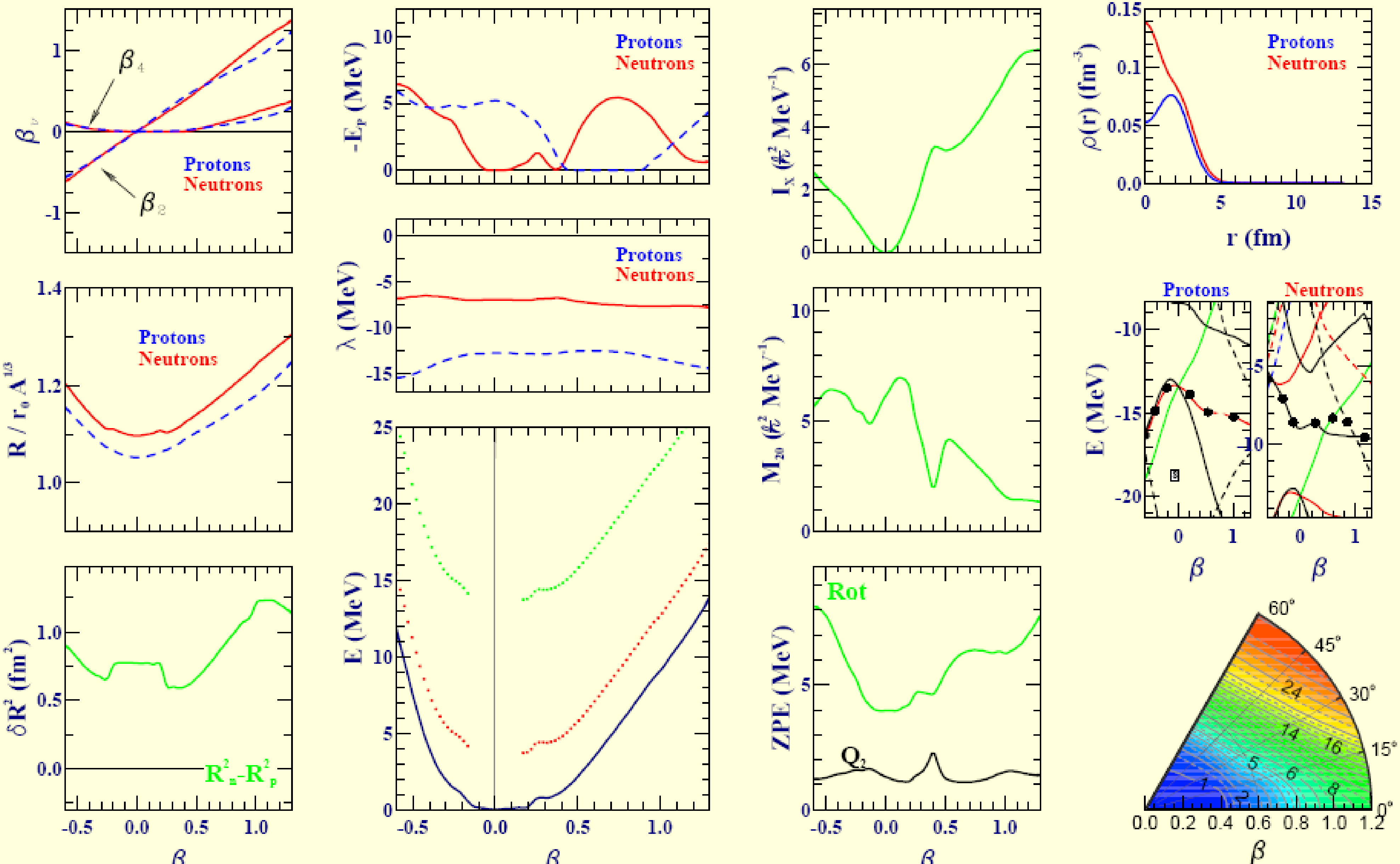

HFB-D1S Bruyères-le-Châtel

$^{30}_{14}Si_{16}$

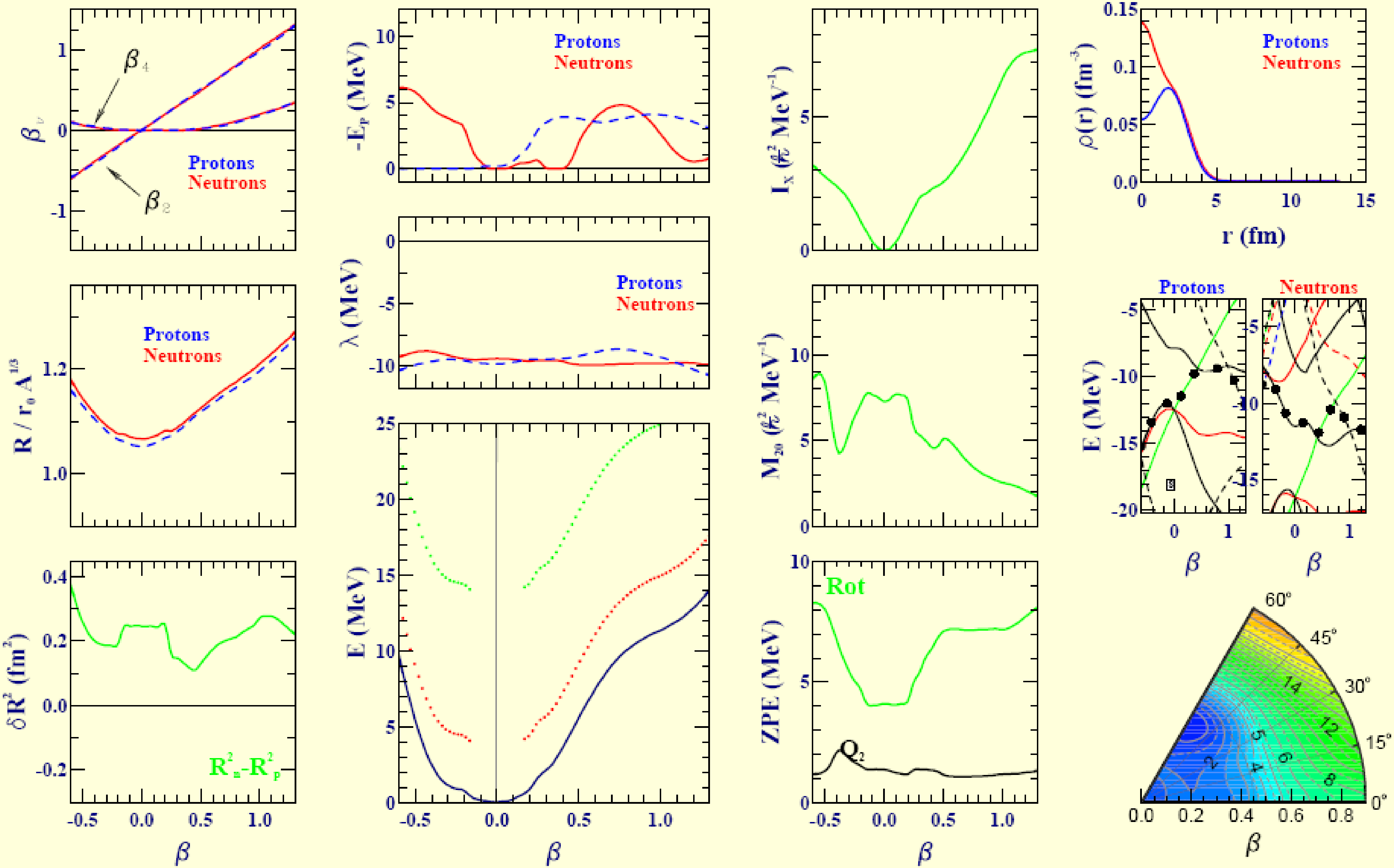

HFB-D1S Bruyères-le-Châtel

energie atomique • energies alternatives

Dipole responses in Neon isotopes

Increasing the neutron number:

- Appearance of PDR and downward shift of the peak
- Increase of fragmentation